Review Article

Liu Yang, Xiaosong Jiang*, Hongliang Sun, Zhenyi Shao, Yongjian Fang, and Rui Shu

Effects of alloying, heat treatment and nanoreinforcement on mechanical properties and damping performances of Cu–Al-based alloys: A review

https://doi.org/10.1515/ntrev-2021-0101
received August 2, 2021; accepted September 30, 2021

Abstract: Cu–Al-based alloys are a kind of new functional material. Due to their unique thermoelastic martensite structure, they have excellent damping performance, which has become a research hotspot in the field of materials science and engineering in recent years. However, the elastic anisotropy and large grain size easily cause a brittle fracture, which is harmful to the mechanical properties of the material. In order to meet the practical needs of engineering, it is an important choice to design Cu–Al-based alloys with excellent mechanical properties and damping performances from the perspective of refining the grain size. When the grain size is small, the effect of fine grain strengthening and interfacial damping can play a role simultaneously to obtain Cu–Al-based alloys with excellent comprehensive properties. In this paper, several common preparation methods of Cu–Al-based alloy are introduced firstly. Then the contributions of researchers in refining grain size from alloying and heat treatment are summarized. Meanwhile, nanomaterials can be used as the reinforcing phase of Cu–Al based alloy, and play a superb role in mechanical properties and damping performances. The purpose of this study is to provide a reference for the further research of structure-function integrated materials with high strength and high damping simultaneously. Finally, the development of Cu–Al-based alloy from the aspects of 3D printing and numerical simulation is prospected.

Keywords: Cu–Al-based alloy, damping performances, mechanical properties, alloying, heat treatment, nanoreinforcement

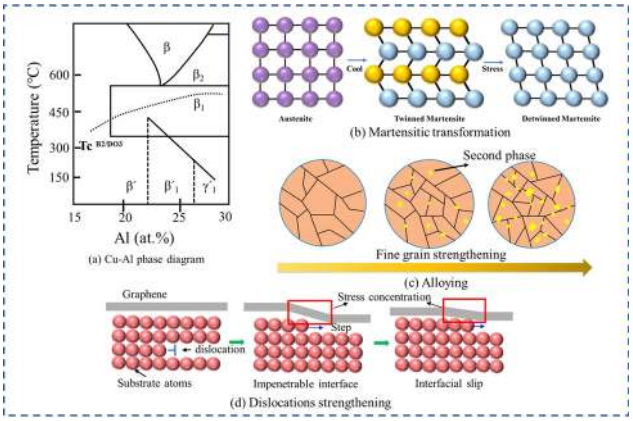

Graphical abstract

1 Introduction

Damping alloys are widely used in automotive, optical equipment, machine tools, and military fields due to their performance of vibration and noise reduction [1–3]. The common damping alloys, such as Mn–Cu alloy, Ti–Ni alloy, and Fe-based alloy, have disadvantages such as expensive raw materials, difficult processing, or strong magnetic field dependence, which limit their applications in some fields [4–6]. Cu–Al-based damping alloys, which have received widespread attention, can effectively avoid the above problems. The unique thermoelastic martensitic

* **Corresponding author: Xiaosong Jiang,** Key Laboratory of Advanced Technologies of Materials, Ministry of Education, Chengdu 610031, China; School of Materials Science and Engineering, Southwest Jiaotong University, Chengdu Sichuan 610031, China, e-mail: xsjiang@swjtu.edu.cn, tel: +86-28-87634177, fax: +86-28-87634177
Liu Yang, Hongliang Sun, Zhenyi Shao: Key Laboratory of Advanced Technologies of Materials, Ministry of Education, Chengdu 610031, China; School of Materials Science and Engineering, Southwest Jiaotong University, Chengdu Sichuan 610031, China
Yongjian Fang: School of Mechanical Engineering, Sungkyunkwan University, 2066 Seobu-Ro, Jangan-Gu, Suwon-Si, Gyeonggi-Do, 16419, Republic of Korea
Rui Shu: Forschungszentrum Jülich GmbH Institut für Energie-und Klimaforschung Plasmaphysik (IEK-4), 52425 Jülich, Germany

structure provides excellent damping capability, making it a highly practical alloy [7]. Its high damping ability originates from a variety of mechanisms, including the migration of point defects and defect pairs, the relaxation of dislocations or the interactions between dislocations and point defects, and the movement of plane interfaces (such as grain boundaries, phase interfaces, and twins) [7,8]. Although Cu–Al-based alloy has excellent damping properties, it has high order, large elastic anisotropy, large grain size, prone to fracture along the crystal, and low fatigue strength, which is not conducive to the improvement of mechanical properties [9–11]. In general, mechanical properties and damping performances have the opposite trend [12]. However, in practical application, the mechanical properties of the damping alloy also need to be guaranteed. At present, researchers have carried out extensive work in obtaining Cu–Al-based alloys with both high damping and mechanical properties by alloying or heat treatment to refine the grain size [13,14].

Alloying or heat treatment can improve the damping properties and mechanical properties by adjusting the microstructure [14,15]. The properties of Cu–Al-based alloys depend mainly on the high-temperature β-phase and are closely related to the type and content of the alloying elements. The improvement of mechanical properties and damping performances by alloying is mainly reflected in the change in the grain size, dispersion strengthening, and martensitic transformation (MT) behavior [14]. Zhang *et al.* [16] investigated the effect of Sm element on the Cu–13Al–4Ni alloy. It was found that with the addition of Sm elements, a single 18R martensite and Sm-rich phase were formed. The formation of the Sm-rich phase increased the Al content in the matrix and reduced the MT temperature. The compressive strength increased from 580 to 1,021 MPa with the addition of 0.5 wt% Sm. This was mainly attributed to the grain refinement that limited the movement of dislocations within the alloy. Kalinga *et al.* [17] added different contents of the B element to the Cu–11.5Al–0.57Be alloy. When the B content was added at 0.15 wt%, the grain size decreased from 1,134 to 50 μm and the compressive strength increased from 216 to 744 MPa; when the B content was increased to 0.2 wt%, the grain size changed to 87 μm and the compressive strength changed to 537 MPa. This was attributed to the agglomeration of coarse B-rich precipitated phases in the base material, which was harmful to the grain refinement. Besides alloying, the thermoelastic martensitic structure of Cu–Al-based alloys indicate that heat treatment is also an effective way to improve the comprehensive properties [18]. Jiao *et al.* [19] found that Cu–Al–Mn aging at 530–620°C could produce controllable precipitation, thus optimizing the microstructure and significantly improving the mechanical properties and damping performances. Therefore, alloying or heat treatment can improve the mechanical properties and damping and broaden the application field of Cu–Al-based alloy.

In addition, nanomaterials have been used as a reinforcing phase due to their nanosize advantage and have shown potential for enhancement of mechanical properties and damping reinforcement of materials. They also show an enhanced damping ratio (0.37–0.42) and a much higher storage modulus (>11.0 GPa). It is promising to further reduce the grain size of Cu–Al-based alloys compared to alloying and heat treatment. Liu *et al.* [20] mentioned that abundant interbundle stick–slip motions throughout the interlocked carbon nanotube (CNT) networks provided excellent energy dissipation capacity for the network. These provide guidance for the development of nanoenhanced phases in Cu–Al-based alloys.

Despite the highly satisfactory results achieved by alloying, heat treatment, and nanoenhancement in Cu–Al-based alloys, several challenges also exist, which are as follows. (1) Currently, the focus is on improving mechanical and damping properties separately through alloying or heat treatment, and there is a lack of research to improve damping and mechanical properties simultaneously. (2) Nanoreinforcement to improve the mechanical and damping properties of other metals has been extensively investigated. Unfortunately, the applications in Cu-based alloys are mainly focused on mechanical properties, while the damping properties are still rare. (3) The functions played by alloying, heat treatment, and nano-enhancement on the performance improvement of Cu–Al-based alloys have not been established in a systematic summary and review. (4) The literature review mainly focused on the improvement of shape memory properties. Sutou *et al.* [21] reviewed that the shape memory properties can be greatly improved by controlling the microstructural factors such as the grain size and organization through heat treatment. There is a considerable lack of review papers on the improved mechanical and damping properties of Cu–Al-based alloys.

Therefore, in order to provide guidance for obtaining functionally and structurally integrated Cu–Al alloys with damping and mechanical properties, the efforts made by researchers to improve the comprehensive properties were in three aspects: alloying, heat treatment, and nanoreinforcement and are systematically reviewed. First, several common preparation methods are introduced. Suitable preparation methods are important to obtain materials with desirable properties. Then, the effects of alloying and heat treatment on the mechanical and damping properties of the alloys are summarized and analyzed, focusing on the microstructure, mechanical properties, MT characteristics,

and damping properties. This article complements the studies of some researchers who have improved the damping and mechanical properties simultaneously from both alloying and heat treatment. In addition, the strengthening mechanism of the nanoenhanced phase is briefly described. Finally, the development of functionally and structurally integrated high-performance alloys from the perspective of 3D printing technology and numerical simulations is discussed and prospected. However, there are a few papers on the application of 3D printing and numerical simulation in Cu–Al-based alloys, so the specific discussion on this aspect in the prospective section is limited.

2 Cu–Al binary phase diagram

In order to better optimize the performance of the target metal, a basic understanding of the phase diagram and crystal structure is required first. According to the Cu–Al phase diagram shown in Figure 1(a), when the atomic content of the Al element is between 20 and 30%, the temperature is higher than 565°C and the alloy is a single β phase with a body-centered cubic structure in the high-temperature region [22,23]. Ordered transitions from β to β_2 and β_2 to β_1 occur during the cooling of the high-temperature β phase to a lower temperature. Even rapid cooling cannot inhibit the occurrence of ordered transitions. The β_2 (CuAl: B2) and β_1 (Cu_3Al: DO3) phases with higher Al content have highly ordered structures [23]. In an equilibrium state, the β phase will undergo an eutectoid reaction at 565°C and decompose into the α phase and γ_2 phase [24]. Between them, the α phase is a solid solution with a face-centered cubic structure (FCC) and the low hardness formed by Al dissolved into Cu. Meanwhile, γ_2 is a solid solution based on electron compounds. It is a kind of hard and brittle phase rich in the Al element. Moreover, its precipitation makes the organization harder and the mechanical properties worse. The rapid quenching from the high-temperature β-phase region can inhibit the occurrence of the eutectic reaction because there is not enough time during the rapid quenching to induce the occurrence of eutectic reactions. As the quenching temperature is further reduced to the martensite phase transformation initiation temperature (M_s), the alloy will start from the austenite phase and transform to the martensite phase; when the temperature is decreased to the end of the martensite-phase transformation temperature (M_f), the transformation of the parent austenite phase to martensite phase ends, and the process is called the martensite-phase transformation process. Martensite is a hard and brittle supersaturated solid solution. From Figure 1(a), it can be observed that the martensitic-phase transition temperature decreases with the increasing Al content, and the type of martensite produced differs depending on the Al content. The three different martensitic structures produced from low to high Al contents are the α′ phase with a disordered FCC structure (3R), the β_1' phase with an 18R structure, and the γ_1' phase with a 2H structure [25]. The β_1' and γ_1' phases inherit the ordered structure of the parent phase and become thermoelastic martensite. When the atomic content of Al is more than 30%, the γ_2 phase will appear to hinder the thermoelastic MT, which is harmful to the damping performance. A sufficient understanding of the Cu–Al binary phase diagram will help us to take reasonable measures to improve the comprehensive performance.

3 The preparation method of the alloy

It is well known that the preparation method of a material determines its microstructure and further affects its properties. Therefore, suitable preparation methods are essential to obtain the desired properties. Several methods for the preparation of Cu–Al-based alloys will be briefly described next. It covers mainly the traditional casting technologies with mature and simple processes, as well as the relatively new mechanical alloying/powder metallurgy technologies of recent years.

3.1 Casting

Casting is one of the most widely used skilled thermal processes for the preparation of alloys [26,27]. The common casting processes, such as investment casting, permanent casting, centrifugal and high-pressure casting, are widely used due to their low cost and net shape advantages [28]. Leu *et al.* [29] prepared the Cu–13.8Al–3.8Ni alloy by induction furnace melting at 900°C, 10 MPa pressure, and an argon atmosphere with strength up to 800 MPa. Duerig *et al.* [30] prepared the Cu–14.2Al–3.2Ni alloy by the casting process with a grain size of about 1,500 μm, fracture stress of 440 MPa, and a fracture strain of 0.6%. The coarse grain structure produced by the conventional casting of Cu–Al-based alloys can limit their potential applications [31]. In the preparation of metals, high-pressure die casting is a manufacturing process with fast mold filling and rapid metal shaping. Its rapid solidification facilitates the production of fine grains [32]. Wang *et al.* [32] successfully

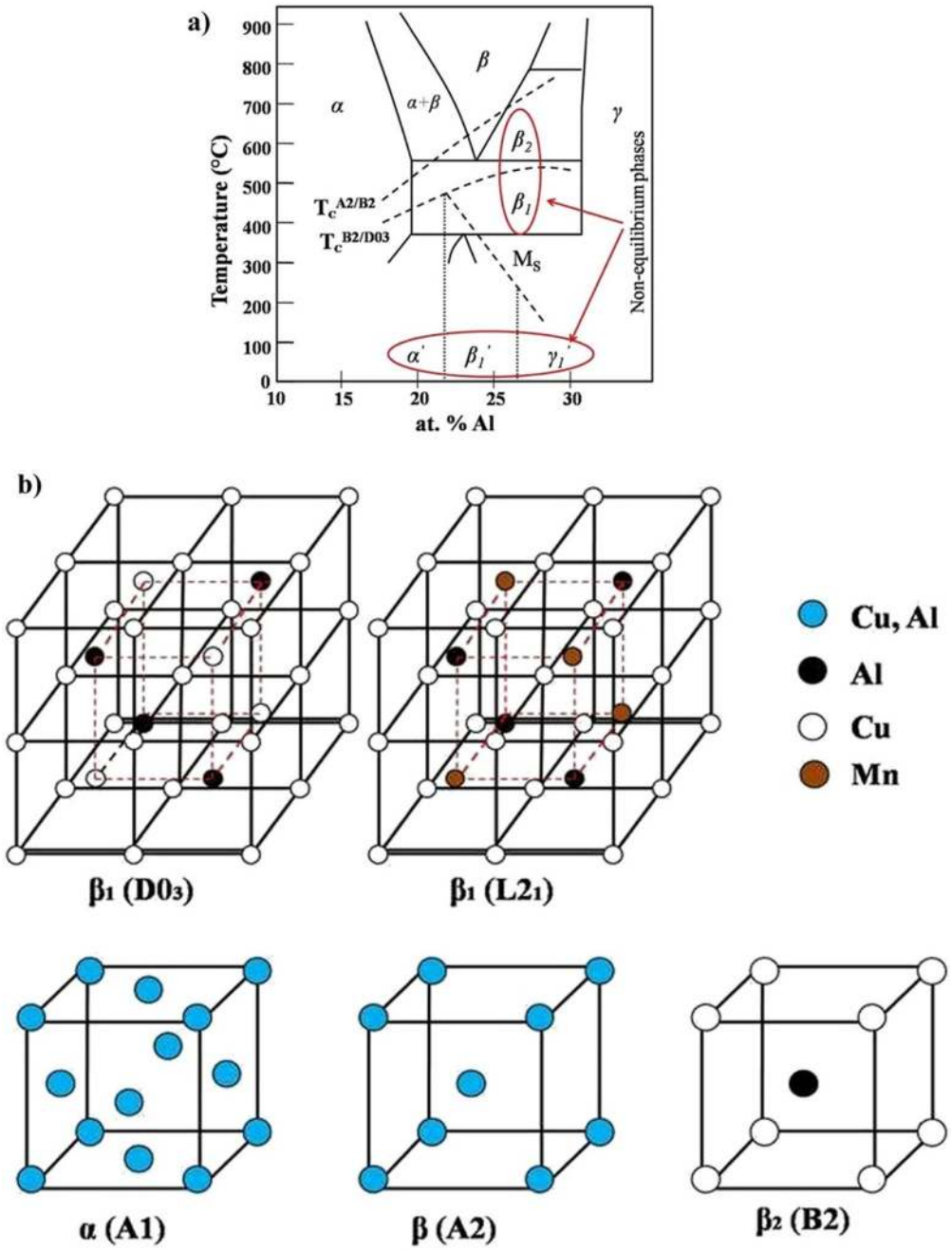

Figure 1: (a) Cu–Al binary phase diagram and (b) the crystal structure of different phases [23].

prepared the AZ91 alloy with reduced grain size and porosity using a high-pressure casting process, indicating that this technique is beneficial for obtaining a more uniform organization. However, the limitations of casting itself are still insufficient to improve the grain size; therefore, adding alloying elements to casting is an effective method to reduce the grain size. Studies showed a significant improvement in the mechanical properties of the Cu–Al–Ni alloy using the addition of group IV elements such as Cr, Ti, Zr, V, and B [33]. This is mainly due to the interaction between the second phase particles generated in the matrix phase and grain boundaries, which leads to grain boundary pinning, thereby reducing the grain size and improving the comprehensive properties of the alloy [31]. It has also been shown that the A8006 alloy after proper heat treatment process can obtain finer microstructure and reduce the adverse effects of

casting due to coarse grain organization [34]. Therefore, the application of casting can be broadened by alloying and changing the heat treatment conditions.

3.2 Powder metallurgy (PM)

Powder metallurgical preparation techniques show their superiority in the grain size and component uniform distribution [35]. The finished products prepared by these techniques are widely used in diversified fields because of their excellent performance and good stability [36,37]. The commonly used powder metallurgy techniques are hot-pressing sintering, hot isostatic pressing sintering, and spark plasma sintering (SPS). Many facts indicated that mechanical alloying had become an effective way to produce a variety of ultrafine powders in the process of powder mixing [38]. Vajpai *et al.* [39] successfully prepared Cu–Al-based alloys with high strength and high ductility by means of powder metallurgy, which was mainly due to the excellent metallurgical bonding between particles promoted by this method. Shafeeq *et al.* [40] also found that the use of a suitable mechanical alloying process in the preparation of Cu–Al-based alloys was beneficial to distribute the elements uniformly and shorten the processing time. Therefore, the combination of mechanical alloying and powder metallurgy sintering can be conducive to obtain the final desired high-performance products.

3.2.1 Mechanical alloying (MA)

MA technology is one of the most important ways to prepare new high-performance materials. The materials prepared by the MA process have a uniform and fine microstructure and dispersed strengthening phase, and their mechanical properties are often better than similar materials prepared by the traditional process [38]. Studies have shown that MA in the preparation of Cu-based alloys can form supersaturated solid solutions to promote particle refinement and improve mechanical properties [41,42]. Its working principle is to use a high-energy ball mill to make all kinds of powders mix evenly in the process of ball grinding, promote the mutual diffusion of elements, and finally, realize the function of mechanical alloying [43,44], as shown in Figure 2(a–b). The appearance of lamellar structure marks the beginning of alloying, as shown in Figure 2(c). In the process of ball milling, the elemental alloying accelerated, and finally, the fine-grain alloy powders were formed [43]. During this process, reasonable selection of milling parameters plays an important role in obtaining an ideal microstructure [44]. Shafeeq *et al.* [40] investigated the effects of ball-milling parameters, such as ball/powder ratio, ball-milling speed, and ball-milling time, on the microstructure and phases of powder metallurgy Cu–Al–Ni–Ti alloys. It was found that grinding in a ball/powder ratio of 40:1 and at a speed of 200 rpm for 40 h achieved a uniform distribution of alloying elements, which were the best conditions for MA. Mayahi *et al.* [45] prepared Cu–13.2Al–4Ni alloy by ball milling and found that high-energy collisions during the mechanical alloying process would lead to an increase in the density of structural defects, lattice strain, and a decrease in the crystallite size. In addition to the above parameters, the choice of ball-milling medium also plays an important role in the final powder formation. Alcohol and stearic acid are usually added as ball-milling media to avoid oxidation and cold welding, whereas alcohol is more readily available and used more widely [46]. In addition, many research works on Cu-based alloy powder metallurgy processing focused on mechanical alloy powder obtained by ball milling [47]. Kaouther *et al.* [48] promoted metallurgical bonding of nanosized Cu–Nb–Al alloy powders after ball milling for 200 h at a speed of 600 rpm, resulting in desirable mechanical strength and ductility of sintered alloys.

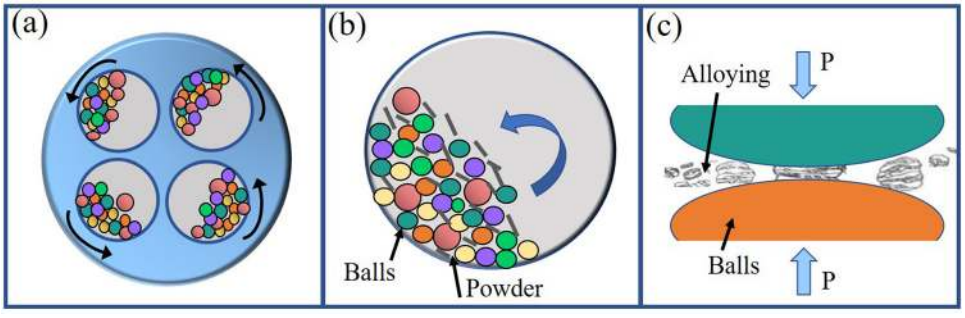

Figure 2: (a) Schematic diagram of ball milling, (b) enlarged view of ball milling tank, and (c) alloying process during ball milling.

In addition, the proper mechanical alloying process is beneficial to the uniform distribution of elements and shortens the processing time [40]. Therefore, MA as an effective way to promote powder alloying is widely used in the whole powder metallurgy field.

3.2.2 Hot-press sintering (HP)

HP is a near-net forming technology for preparing highly compact alloys [47,49]. The method also has the advantages of high production efficiency and uniform product organization [50]. Xiao *et al.* [51] prepared a Cu–11.9Al–5-Ni–2.2Mn alloy with high density and uniform element distribution by HP technology under the following conditions: temperature, 950°C; pressure, 40 MPa; holding time, 120 min; and vacuum degree, 10^{-1} Pa. Liu *et al.* [52] obtained a TiNiNb alloy with a relative density of 98.8% under the hot-pressing conditions: temperature, 900°C; pressure, 35 MPa; vacuum degree, 1.6×10^{-3} Pa; and holding time, 1 h. Rodríguez *et al.* [53] prepared a Cu–14.2Al–4.2Ni alloy with good ductility after hot pressing at 900°C for 1 h. Vajpai *et al.* [54] prepared a Cu–Al–Ni alloy with reduced grain size and improved fracture strength by this method, which is salutary to the improvement of the comprehensive properties of the alloy. In addition, the selection of hot-pressing temperature has an important effect on the properties of the alloy [55]. Wakai *et al.* [56] also showed in their study that extremely high hot-pressing temperature will lead to excessive growth of grains, resulting in weakening of the effect of fine-grain strengthening. Wang *et al.* [57] prepared a Ti–22Al–25Nb alloy by vacuum hot-pressing sintering process and found that the alloy showed good comprehensive properties under the sintering process of 1,250°C, with the tensile strength and elongation reaching 620.53 MPa and 7.44%, respectively. Therefore, it is of great significance to select suitable technology in the process of HP to obtain materials with ideal properties.

3.2.3 Hot isostatic pressing (HIP)

HIP is another important method to obtain high-performance compact materials. It is a process of applying equal pressure and high temperature to the product in all directions and obtains the process products with a high internal density under the condition of high temperature and high pressure [58–60]. By adjusting the experimental parameters of the technology, temperature, and pressure, the microstructure and performance of the final prepared material can be controlled [61–63]. Cai *et al.* [61] prepared a compact and defect-free Ti6Al4V titanium alloy after HIP treatment at a temperature of 900–930°C and a pressure greater than 100 MPa. The strength and fatigue life of the alloy were significantly improved. Ran *et al.* [58] used hot isostatic pressing at 520°C and 100 MPa for 2 h to prepare an A356 alloy with a fine grain structure, which significantly reduced the porosity of the sample and improved the strength of the alloy. Jiang *et al.* [64] achieved complete densification and homogenization of the $Cu/Ti_3SiC_2/C$/graphene nanocomposites between the direction parallel and perpendicular to the pressure direction through hot isostatic pressing. Many studies have shown that the materials prepared by this method generally have a uniform fine grain structure, good process performance, and mechanical properties [65–67]. Therefore, due to its superiority, this technology has been widely used in many fields such as machine manufacturing, aerospace, and aviation.

3.2.4 SPS

With the increasing types and demands of new functional materials, SPS has been widely used as a new technology [68–70]. SPS has the characteristics of fast heating speed, short sintering time, controllable structure, energy saving, and environmental protection, making it suitable for the preparation of metal materials, ceramic materials, and composite materials [71,72]. The technology is affected by sintering temperature, holding time, pressure, and current, and the powder can be rapidly prepared into dense blocks with appropriate process parameters [73]. Richard *et al.* [74] obtained Cu–13.01Al–3.91Ni–0.37Ti–0.24C alloys with excellent properties by using SPS technology, which provided rapid heating for powder sintering through the graphite mold and the alternating current, and the sample placed therein at a maximum uniaxial pressure of 99.5 MPa. Eze *et al.* [75] prepared a Cu–Ti-based alloy with a strength of 749 MPa through SPS at 650°C and 50 MPa for 5 min. Qiang *et al.* [76] studied the size and distribution of reinforcers in the matrix of mechanical alloying and powder metallurgy processes, as shown in Figure 3. It was found that the hard chromium particles were further deformed after mechanical alloying, and the broken chromium was then embedded into the soft copper particles, regardless of the pretreated state of the powder. Finally, the material with high mechanical properties was obtained by SPS. In addition, Tan *et al.* [77] successfully

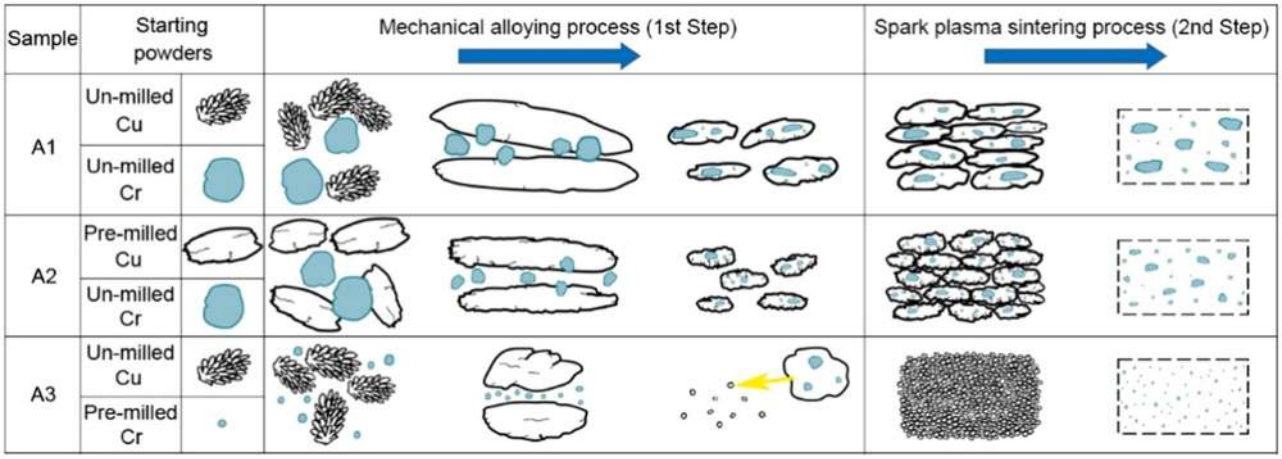

Figure 3: Size and distribution of reinforcement in the matrix after mechanical alloying and SPS processes [76].

prepared a high density and high strength 7056 Al alloy by SPS technology and confirmed that the diffusion of elements between the aluminum alloy matrix and the reinforcing body occurred during the SPS process. As a novel technology, SPS plays a guiding role in efficiently obtaining high-quality materials [78,79].

3.3 Summary of the preparation methods

The schematic diagram of the commonly used casting, hot pressing, hot isostatic pressing, and SPS processes is shown in Figure 4. The casting shown in Figure 4(a) is mainly a method of filling and forming the cavity by

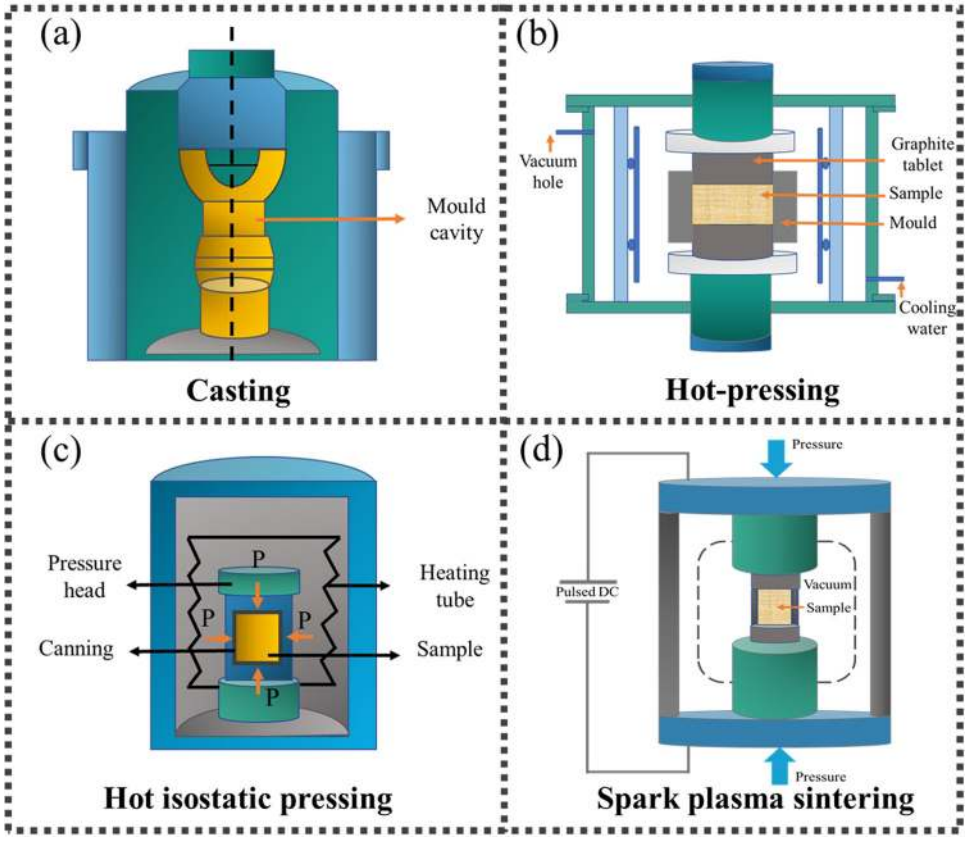

Figure 4: Preparation process of alloy: (a) casting, (b) hot-pressing sintering, (c) HIP, and (d) SPS.

metallic liquid under the action of other external forces. As shown in Figure 4(b), HP is to form and sinter the material by adding dry powder into the mold, and then pressure and heat are applied in a uniaxial direction. The HIP as shown in Figure 4(c) is a method in which the material is formed under the combined action of high temperature and pressure, and the material being processed is pressed equally in all directions. SPS is a method of forming by loading a powder such as metal into a mold and applying specific sintering power and pressing pressure to the sintered powder using upper and lower die punches and energized electrodes, as shown in Figure 4(d). In summary, casting and powder metallurgy are two completely different processes. Casting is a phase change from liquid to solid for molding and is subject to defects such as porosity and shrinkage that are difficult to overcome. PM uses the fusion of low-melting-point materials between particles for molding and usually a more uniform and finer microstructure is obtained. Therefore, in the application of Cu–Al-based alloys, powder metallurgy techniques are more widely used in order to obtain a more uniform and finer grain structure.

4 Alloying and heat treatment

4.1 The influence of alloying elements

As one of the effective methods to improve the properties of alloys, alloying has been favored by many experts [80–84]. The selection of alloying elements generally needs to meet the following aspects [85]: (1) should have low solubility and not easily soluble in the matrix alloy; (2) should combine with other elements in the substrate to generate fine compounds; (3) should be able to form intermetallic compounds to change the content of the chemical composition of the substrate, thereby affecting the phase transition temperature; and (4) capable of maintaining solid solution and increase the stability of β phase. In addition to common elements, rare earth elements, due to their active properties, can easily combine with the elements in the alloy to form high melting point compounds, disperse in solution and act as heterogeneous nucleation to increase the nucleation rate [86]. Moreover, the rare earth elements enriched in the matrix alloy will hinder the expansion of grain boundaries and reduce the growth rate of grains to refine grains [86]. Therefore, the mechanical properties and damping performances of the alloy can be improved by adding appropriate elements from the aspects of grain refinement, dispersion strengthening, influence on phase transformation behavior, and martensite behavior [87,88].

4.1.1 The influence of alloying elements on the microstructure

As well known, the microstructure of the material will be affected by the composition and then affects the performance of the material [89]. This was mainly because the addition of alloying elements had low insolubility and would generate fine compounds due to its reactions with the parent phase elements, thus hindering the growth of grains and changing the microstructure of the alloy [90]. The properties of Cu–Al-based alloys mainly depend on the high-temperature β phase, and the behavior of martensite also strongly depends on the type and content of the alloy. Their properties are largely affected by the grain size, phase composition, and thermoelastic martensite [88].

Many studies have shown that modulating the microstructure of alloys by alloying is a very effective method [89–91]. Saud *et al.* [88] added Mn, Ti, and Co elements to the Cu–11.9Al–4Ni alloy, and the alloy was affected by the accumulation and precipitation phases at grain boundaries, which hindered the grain growth and reduced the grain sizes to 450, 650, and 320 μm, respectively. Zhang *et al.* [91] found that the grain size decreased significantly after adding different contents of Nb to the Cu–13Al–4Ni alloy, which was mainly related to the newly formed (Al,Ni)Cu_4Nd. In addition to the above elements, Ti is often added to alloys to improve the microstructure of substrates due to its low solid solubility in the β phase (less than 0.05 wt%), which tends to form fine and evenly distributed precipitates to refine the grain size [92–94]. Saud *et al.* [90] added different contents of the Ti element to the Cu–Al–Ni alloy; the decrease of the grain size and the increase of the precipitate phase reduced the mobility of the interface and changed the morphology of martensite. Similarly, Sampath [89] added Ti and Zr to Cu–Al–Ni, and the fine precipitates rich in Ti and Zr elements prevented the nucleation and growth of grains through the action of pinning. These results indicate that alloying plays an important role in microstructural adjustment.

In addition to the addition of alloying elements, numerous rare earth elements can also obtain good properties [95]. Rare earth elements such as Ce, Gd, Sn, and Te have been widely used in alloys and satisfactory results have been obtained [96–98]. The addition of rare earth elements in Cu–Al alloys has also been developed in

recent years. Yang *et al.* [99] found that the addition of 0.43 wt% mixed rare earth to the Cu–Zn–Al alloy reduced the grain size of the alloy. Dalvand *et al.* [95] added 0.04 wt% rare-earth elements (Ce + La) to the Cu–12Al–3Ni–0.6Ti alloy, resulting in a reduction of about 30% in the average grain size due to the formation of rare-rich precipitated phases, as shown in Figure 5. Meanwhile, the addition of Gd and other alloying elements in the Cu–Al alloy also plays a crucial part in refining the grain size [100].

Apart from the change in the grain size, the phase composition of the alloy is also affected by the alloy composition. The lattice parameters of the orthogonal element of the 18R structure martensite with thermoelastic effect can be expressed by ref. [88].

$$\frac{1}{d^2} = \frac{1}{a^2}\left[\frac{h^2}{\sin^2\beta}\right] + \frac{k^2}{b^2} + \frac{1}{c^2} + \left[\frac{l^2}{\sin^2\beta}\right] - \frac{2hl\cos\beta}{ac\sin^2\beta}, \quad (1)$$

where d is the distance between the planes; (h, k, l) is the Miller index; a, b, and c are the axis length; and β is the interaxial angle.

Zhang *et al.* [100] found that the Cu–Al–Ni alloy with a Gd element was mainly composed of 18R martensite and the second phase, and the 18R martensite with high thermoelastic behavior and controlled growth in the adaptive group existed in a typical zigzag morphology [86]. Zhang *et al.* [91] added different Nb contents to the Cu–13Al–4Ni alloy, in addition to the 18R structure and 2H structure martensite, a newly formed (Al, Ni) Cu_4Nd phase appeared in the substrate, as shown in Figure 6. Sari [82] found that γ_1' and β_1' martensite appeared in the Cu–11.9Al–3.8Ni alloy with the addition of 2.5 wt% Mn. γ_1' martensite came out in the coarse variant, while β_1' martensite showed up in a typical zigzag shape. With the addition of Ag in the Cu–Al–Ni alloy [81], the Ag element is easily diffused into the matrix to react and form the precipitate phase, which will promote the formation of 18R martensite. Yildiz [101] studied the effect of Ta content on the microstructure of the Cu–12.4Al–4Ni–1Mn alloy. The results showed that with the addition of the Ta content, the microscopic composition of the alloy changed from 18R and 2H double martensite phase to 18R single martensite

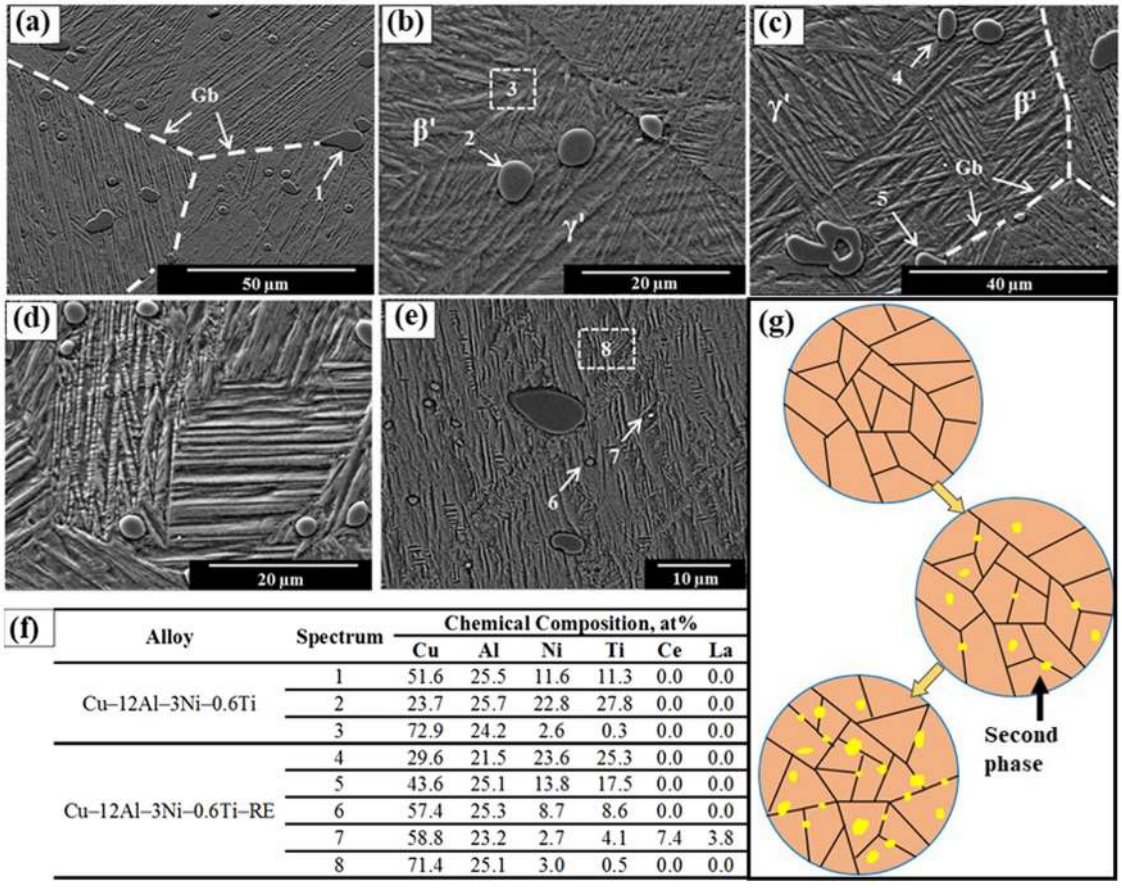

(f)

Alloy	Spectrum	Chemical Composition, at%					
		Cu	Al	Ni	Ti	Ce	La
Cu–12Al–3Ni–0.6Ti	1	51.6	25.5	11.6	11.3	0.0	0.0
	2	23.7	25.7	22.8	27.8	0.0	0.0
	3	72.9	24.2	2.6	0.3	0.0	0.0
Cu–12Al–3Ni–0.6Ti–RE	4	29.6	21.5	23.6	25.3	0.0	0.0
	5	43.6	25.1	13.8	17.5	0.0	0.0
	6	57.4	25.3	8.7	8.6	0.0	0.0
	7	58.8	23.2	2.7	4.1	7.4	3.8
	8	71.4	25.1	3.0	0.5	0.0	0.0

Figure 5: SEM micrographs of the alloys: (a and b) Cu–12Al–3Ni–0.6Ti alloy, (c–e) Cu–12Al–3Ni-0.6Ti–RE alloy, (f) table of element distribution in numbered areas in (b and e), and (g) simple schematic diagram of second phase precipitation [95].

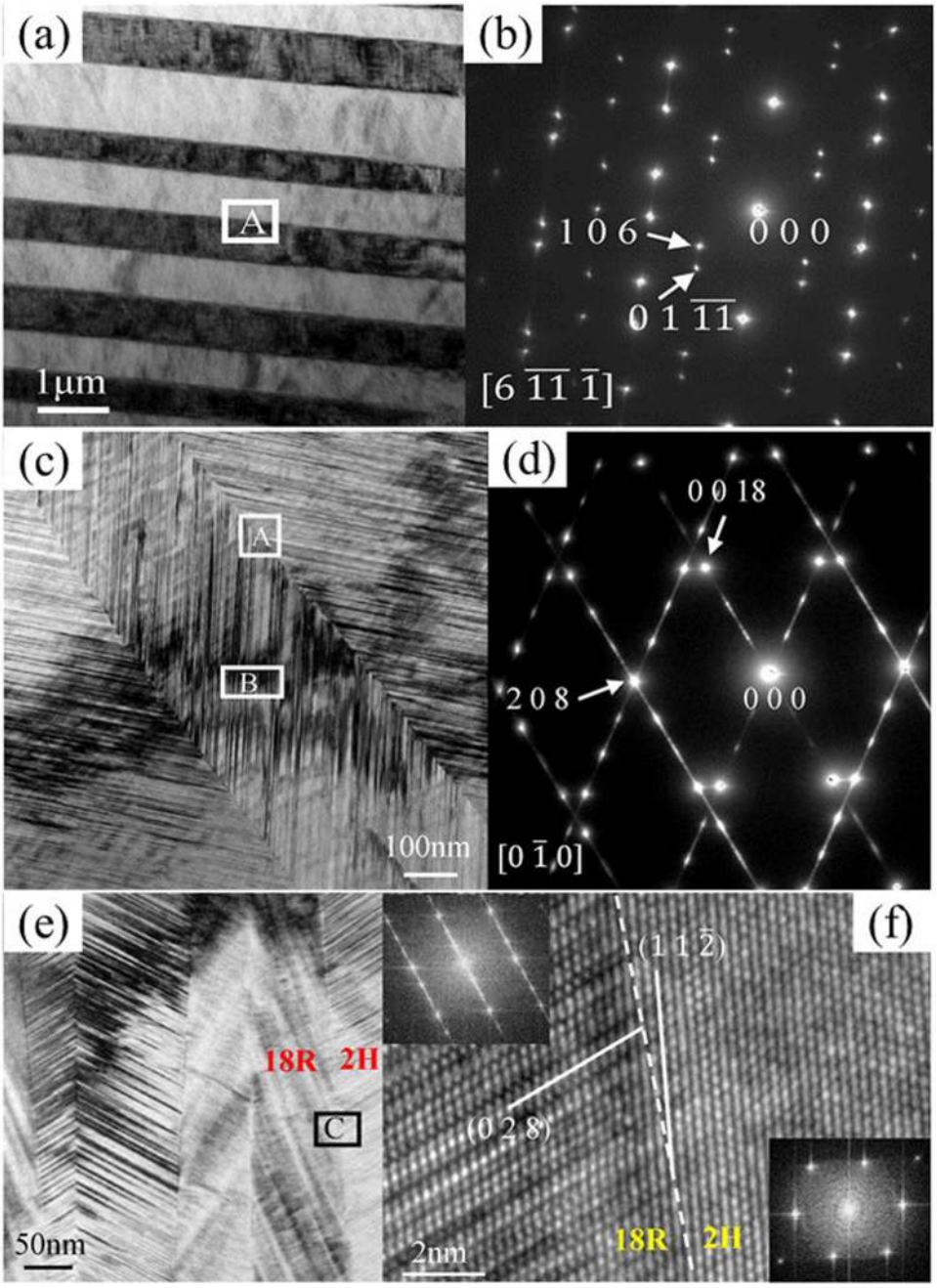

Figure 6: TEM images of Cu–13.0Al–4.0Ni–1Nd alloy: (a) bright field image, (b) electron diffraction of region A in (a), (c) bright field image, (d) electron diffraction of region A in (b), (e) bright field image, and (f) electron diffraction of region C in (e) [91].

phase, and the volume fraction of the Ni_2Ta phase increased with the increase of the Ta content. These changes in the phase composition are of great significance for obtaining rational comprehensive properties of alloys.

It must be noted that electron probe X-ray micro-analysis (EPMA) is also one of the commonly used methods for modern microscopic analysis in the study of alloys. It has great advantages in the quantitative analysis of elements, distribution of trace elements, and analysis of inclusions and precipitated phases. It is even possible to measure compositional differences in microscopic phase distributions at the micron or even nanometer scale [102]. Lin *et al.* [103] found that in addition to the second phase discovered by SEM, the Al_6Fe phase was also detected when EPMA was used to measure the corrosion resistance of trace Sc and Y in the high-conductivity cold-drawn Al–0.2Ce base

alloy. Shang *et al.* [104] used EPMA to successfully determine whether Mg content can be ignored in the composition calculation in the study of the second phase of the AZ31 magnesium alloy containing Ca, Si, and Ce. Meanwhile, it can fully identify each phase present in the inclusions. The composition of $Al_9Cu_{11.5}$ and $Al_{0.939}Cu_{0.987}$ phases is very close and they were usually identified as the AlCu phase in previous studies. However, Liu *et al.* [105] successfully differentiated them using EPMA. In addition, in the analysis of the second phase entrapped in the tungsten wire, it was found that the elements Y, La, and Hf, which cannot be detected in the second phase by EDS, could be detected by using EPMA [106]. EPMA can also detect the type of deviations of elements on martensite to determine the cause of martensite formation, which is not obvious if the energy spectrum detection is used [107]. In conclusion, EPMA helps to improve the precise positioning of the analysis area and the accuracy of the analysis. The analysis results are highly intuitive and will play an increasingly important role in future trace analysis. Therefore, researchers are encouraged to use EPMA for more accurate microzone analysis in future studies involving alloys.

In addition to the use of alloying elements, the addition of inoculants will significantly affect the microstructure and performance of the alloy while refining grains [108–110]. In order to achieve a better optimization effect, researchers cleverly combined alloying elements and grain refiners and studied the effect of their combined action on the alloy. Ding *et al.* [111] made use of the compound refining effect of the $Cu_{51}Zr_{14}$ incubator and Ti element to significantly refine the grain size of the Cu–Al–Ni alloy and improve the properties of the alloy. The inoculant refines the grain mainly by providing a heterogeneous nucleation core to the melt, while Ti refines the grain mainly by preventing grain growth. In addition, researchers also showed that the orientation relationship between the inoculant and the matrix alloy, the atomic matching, and the interface bonding state had significant effects on the refining effect of the alloy [112]. When the matrix alloy and the inoculant had similar atomic arrangement rules at the interface, the wettability and lattice matching between the two were better, which could achieve a good refining effect [113,114]. Figure 7 shows a simple schematic diagram of lattice matching between the matrix alloy and the inoculant. Wang *et al.* [115] reported that the morphology and the stress state of the second phase/matrix alloy interface depend on the difference in physical properties between the base alloy and the second phase. The different thermal expansion coefficients between the two phases would cause different shrinkage of the specimen during the solidification and cooling process, resulting in internal stress and leading to the appearance of the second phase. Moreover, only inoculant particles with appropriate average size had the best refining effect on the target alloy, while inoculant particles with inappropriate size might be pushed to the grain boundary [116]. Therefore, to obtain better performance, factors such as lattice matching degree and interface state between the inoculant and matrix alloy are very important in the selection of the inoculant [117–119].

4.1.2 The influence of alloying elements on mechanical properties

The mechanical properties of alloys are usually controlled by many parameters, such as the grain size, vacancies, grain boundaries, phase sequence, precipitation, structural morphology, and dislocations [82]. To maintain the continuity of strain, Cu-based alloys with large elastic anisotropy are usually prone to stress concentration [120]. Meanwhile, the coarse grain size and the grain boundary segregation of impurity elements make

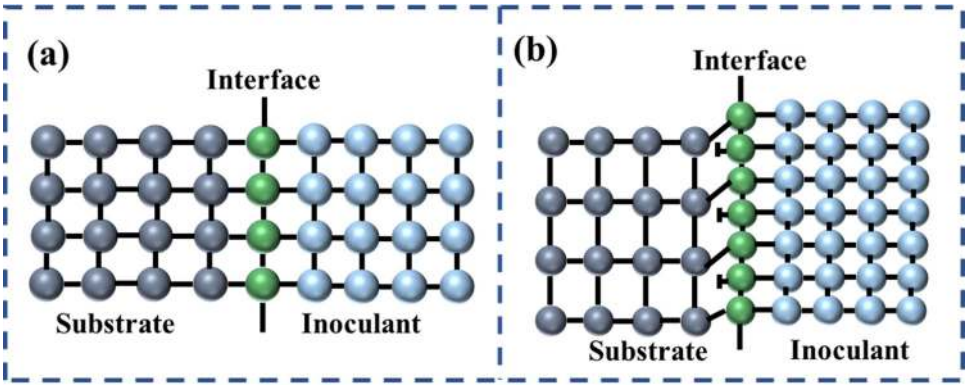

Figure 7: Schematic diagram of lattice matching between the base alloy and the wetting agent. (a) Coherent interface (b) semi-coherent interface.

the alloy prone to brittle fracture. In order to improve the above problems, researchers have achieved good results in improving the properties of the alloy by achieving fine-grain strengthening through alloying [80–82]. It is worth noting that grain refinement can significantly affect the strength of the alloy [121,122]. The Hall–Petch formula gives the relationship between the yield strength and the average grain diameter, as shown in equation (2) [117]:

$$\sigma_s = \sigma_0 + KD^{-1/2}. \quad (2)$$

Among them, σ_s is the yield strength of the alloy, σ_0 is the resistance to deformation within the grain, K is the influence coefficient of the grain boundary structure on the deformation, and D is the average diameter of the grains. It can be seen from the above formula that the yield strength of the alloy is closely related to the grain size. As the grain size decreases, the yield strength increases, that is, the fine-grain strengthening is confirmed.

With the addition of the Nb content in the Cu–13Al–4Ni alloy, the grain size of the alloy was reduced, and the pinning effect of the second phase (Al, Ni) Cu_4Nd prevented the movement of dislocations, resulting in the increase of the compressive strength from 580 to 787 MPa, and finally reaching 940 MPa [91]. The compression fracture strength of the Cu–Al–Ni alloy is obviously improved by adding Gd and Fe to the alloy because the grain boundary is strengthened [112]. Moreover, some results showed that the addition of appropriate alloying elements could improve the ductility by strengthening grain boundaries without forming γ-phase boundaries [113]. Besides, other researchers also made some progress in this regard. After the addition of different Gd elements to Cu–13.0Al–4.0Ni, the newly formed $AlCu_4Gd$ hindered the growth of grains, refined the grains, and improved the mechanical properties of the material [100]. The fracture strength of the alloy was significantly increased from 580 MPa to 1,200 MPa. The hardness of the Cu–14Al–4.5Ni alloy increases with the addition of the hard substance Ce, which is difficult to dissolve in the matrix, and the effect of grain refinement is achieved so that the strength of the alloy is also improved [114]. When 2.5 wt% Mn is added to the Cu–11.9Al–3.8Ni alloy, the grain refinement is realized, and the high fracture strength and fracture strain are obtained [85]. Similarly, the addition of Ag in Cu–Al–Ni also increases the fracture strength of the alloy and changes from the brittle fracture mode to the mixed fracture mode. It indicates that Ag precipitation at the grain boundary, on the one hand, impedes the dislocation movement; on the other hand, it reduces the stress concentration and improves the mechanical properties of the material [81]. In addition, Dalvand *et al.* [95] found that when Ti and rare earth elements were added to the Cu–12Al–3Ni–0.6Ti alloy, the fracture showed a combination pattern of brittle fracture and ductile fracture, as shown in Figure 8. It was found that the dimples appeared around the Ti element and rare earth rich elements, which inferred that the addition of alloying elements and rare earth elements were likely to delay the intergranular fracture and improve the ductility of the alloy.

4.1.3 The influence of alloying elements on the martensite transformation

The typical thermoelastic martensite structure of Cu-based alloy highlights a number of properties. The alloy is mainly composed of a high-temperature austenite phase and a low-temperature martensite phase. Martensite is the product of the austenite parent phase under extreme cooling or stress-induced under high-temperature conditions [123]. The phase transition temperatures of the two are A_s, A_f, M_s, and M_f, respectively, where A_s stands for the beginning temperature of the austenitic transformation, A_f for the ending temperature of the austenitic transformation, M_s for the beginning temperature of MT, and M_f for the ending temperature of MT. The value of $A_s - M_s$ represents the hysteresis degree [123]. The phase transition temperature is affected by the element and element content, and the slight deviation of the composition will cause the increase and decrease of the alloy phase transition point [124]. The relationship between M_s and components is shown in equation (3) [24]:

$$M_s = C + \sum a_i A_i(K), \quad (3)$$

where C is a constant; A_i is the number of elements; and a_i is a constant corresponding to the appropriate quantity of the element.

For the convenience of calculation, the typical phase transition temperature of the Cu–Al–Ni alloy is calculated by equation (4) [24]:

$$M_s(°C) = 2{,}020 - 45 \times (wt\%Ni) - 134 \times (wt\%Al). \quad (4)$$

In addition, the dependence of the M_s temperature on the composition is related to the free energy difference between the parent phase and martensite. According to the Salzbrenner and Cohen equilibrium temperature calculation formula, the temperature T_0 at which the chemical energies of the austenite and martensite phases are equal can be calculated. As shown in equation (5) [125],

$$T_0 = \frac{1}{2}(M_s + A_f). \quad (5)$$

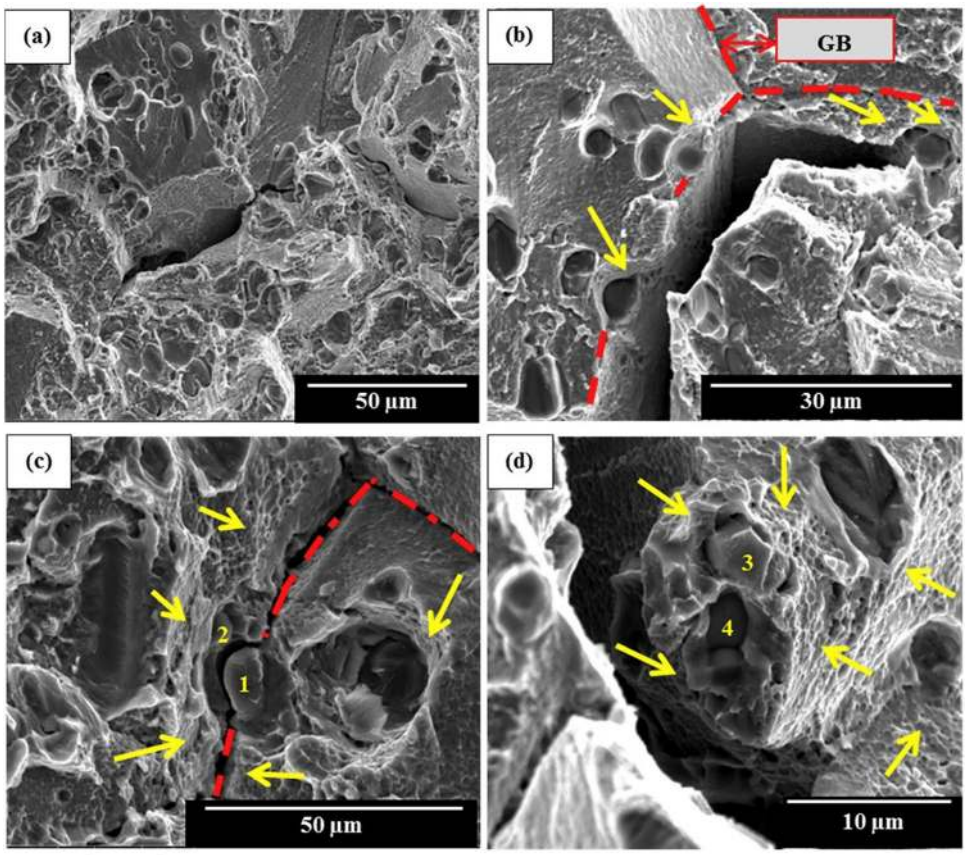

(e)

Spectrum	Chemical Composition, at%					
	Cu	Al	Ni	Ti	Ce	La
1	29.9	26.3	19.9	23.9	0.0	0.0
2	55.6	35.4	3.0	0.9	3.5	1.6
3	29.8	23.5	19.5	27.2	0.0	0.0
4	60.5	30.9	3.5	1.0	2.9	1.2

Figure 8: (a–d) SEM images of tensile fracture of Cu–12Al–3Ni–0.6 Ti–Re alloy and (e) EDS microscopic analysis results of fractured numbering points [95].

The phase transformation process of the alloy can be reflected by the different scanning calorimetry (DSC) curves, in which the endothermic peak and exothermic peak can be observed. The endothermic peak refers to the reverse MT during heating, and the exothermic peak refers to the MT during cooling. The main reason for the curve change is the influence of thermodynamic parameters, such as the change in enthalpy and entropy. The total area under the peak gives the change in enthalpy, ΔH, and the entropy of the intermediate phases can be calculated by dividing the change in enthalpy by the equilibrium temperature (T_0). It has been found that the enthalpy of martensite to austenite transformation is greater than that of reverse transformation, indicating that the forward transformation requires more heat than the reverse transformation [126]. Taking the anti-martensitic process as an example, the change in entropy can be calculated according to equation (6) [127]:

$$\Delta S_{M\to A} = \frac{\Delta H_{M\to A}}{T_0}, \tag{6}$$

where ΔS is the change in entropy; ΔH is the change in enthalpy; and T_0 is the equilibrium temperature between martensite and austenite phases. The higher the entropy, the more martensite will be transformed, which is beneficial to the damping performances and practical application of the alloy.

At the same time, the change in entropy will also affect the heat capacity of the alloy. The specific heat capacity can be calculated by equation (7) [128]:

$$C_P = \frac{1}{m}\frac{\delta Q}{\mathrm{d}T} = \frac{1}{m}\frac{(\delta Q/\mathrm{d}t)}{(\mathrm{d}T/\mathrm{d}t)} \tag{7}$$

where $\mathrm{d}Q/\mathrm{d}t$ is the heat flow of the DSC curve, m is the mass of the sample, $\mathrm{d}T/\mathrm{d}t$ is the heating rate of the sample, T is the temperature, and t is the time.

Therefore, the grain size and thermodynamic parameters of the alloy have an important effect on the transformation temperature of the alloy. Zhang *et al.* [91] found that the resulting (Al,Ni)Cu_4Nd changed the Al content in the matrix alloy and reduced the MT temperature after adding different contents of Nb element to the Cu-14Al–3Ni alloy. Adnan *et al.* [114] added different contents of Ce to the Cu–14Al–4.5Ni alloy, and the phase transition temperature of the alloy moved toward the endothermic direction. Waitz *et al.* [129] reported that grain boundaries in TiNi-based alloys can provide an additional transition energy barrier for the martensitic transition, thereby reducing the martensitic transition temperature. When 2.5 wt% Mn is added to the Cu–11.9Al–3.8Ni alloy, the phase transition temperature decreased due to grain refinement and the stable parent phase, and multiple peak values appeared due to the transition of multiple interfaces [82]. Mallik and Sampath [128] showed that after adding Zn and Ni to Cu–Al–Mn, since the two elements can dissolve in Cu to form a solid solution, the hardening of the solid solution increased the phase transition temperature. Due to the low solubility of Fe, Cr, Ti, Si, Mg, and Cu, fine precipitate particles were formed to reduce the phase transition temperature. At the same time, the addition of Pb would hinder the phase transition due to the formation of a large amount of precipitate phase. In addition, the addition of alloying elements also affected the thermodynamic parameters. The enthalpy and entropy of the Cu–11.9Al–4Ni alloy phase transition increased gradually with the addition of the Ti element. When the Ti element content reached 1 wt %, the enthalpy and entropy reached the maximum value. Because the thermal stability of the alloy was inversely proportional to the enthalpy value, the stability of the alloy decreased gradually with the addition of the Ti element. This might be related to the content and behavior of the precipitated phase and the morphology of martensite [90].

4.1.4 The influence of alloying elements on damping performances

As a new kind of functional material, Cu-based alloy has become a research hotspot due to its excellent damping performance. In addition to the dissipated energy caused by the hysteretic motion of defects and dislocations, its high damping capacity is also due to the frictional energy dissipated between martensite/martensite interfaces, parent/martensite interfaces, and twin interfaces [5,130]. Damping characteristics are generally composed of the following three parts, as shown in equation (8) [131]:

$$\mathrm{IF}(T) = \mathrm{IF}_{\mathrm{Tr}}(T) + \mathrm{IF}_{\mathrm{PT}}(T) + \mathrm{IF}_{\mathrm{Int}}(T), \tag{8}$$

where $\mathrm{IF}_{\mathrm{Tr}}(T)$ is the transient damping, which only appears in the heating or cooling process; $\mathrm{IF}_{\mathrm{PT}}(T)$ is a phase change term, which is closely connected to the process of phase change, leading to the appearance of peaks in the damping spectrum; and $\mathrm{IF}_{\mathrm{Int}}(T)$ is an intrinsic term, which is related to the background internal friction of the parent phase and the new phase.

The maximum damping value of the alloy appears in the thermoelastic martensite transformation temperature range since there is usually plenty of transformed martensite in this temperature range [93]. The peak value within the phase transition region can be expressed by equation (9) [131]:

$$\tan\delta \sim \frac{1}{\omega}\frac{\mathrm{d}\varphi(V_{\mathrm{m}})}{\mathrm{d}V_{\mathrm{m}}}\frac{\mathrm{d}V_{\mathrm{m}}}{\mathrm{d}T}\frac{\mathrm{d}T}{\mathrm{d}t}, \tag{9}$$

where V_{m} is the volume fraction of the transformation martensite, ω is the angular frequency where stress is applied, and $\varphi(V_{\mathrm{m}})$ is a monotonic function of the volume fraction of the phase transition. Assuming that $(\mathrm{d}\varphi/\mathrm{d}V_{\mathrm{m}})$ is a constant for all thermoelastic martensite, the equation states that the damping capacity of the alloy is proportional to the number of transformed martensite.

Therefore, both the amount of martensite and the density of the different phase interfaces play a vital role in the damping properties [93]. Increasing the interfacial density can be achieved by refining the grain size and martensite, for which researchers have done tremendous research. According to the Cu–Al binary phase diagram, the content of the Al element plays an important role in the properties of the alloy. For example, an increase in the Al content decreases the damping properties. This is due to the decrease in the amount of martensite and the formation of γ_2 that inhibits the mobility of the interface [131]. Sutou *et al.* [132] reported that the addition of B, Ni, and Si elements can significantly reduce the grain size of the Cu–Al–Mn-based alloy, which is very important for enhancing the damping performance. After adding the Co element to the Cu–Al–Ni alloy, due to the increase in the number of grain boundaries, there was compressive stress at the adjacent interface, which was pernicious to the movement of the interface [133]. In addition, the addition of rare earth elements can also improve the damping characteristics of the alloy. Lu *et al.* [86] showed

that the appropriate content of Ce elements can significantly improve the damping properties of the alloy, as shown in Figure 9. The results showed that the alloy obtained the best damping performance when the Ce content was 0.05 wt%.

4.1.5 Summary of the alloying mechanism

Alloying plays a crucial role in the adjustment of the microstructure, which in turn is closely related to the properties of the alloy. The common alloying elements or rare earth elements are added for the purpose of reducing the large grain structure of the Cu–Al-based alloy itself and thus optimize the comprehensive properties.

Fine-grain strengthening, a common strengthening mechanism, has the characteristic of simultaneously improving the strength and ductility of the alloy [86]. This is because the increase in the number of grain boundaries after grain refinement can effectively prevent dislocation movement and crack extension [86]. When the material resists stress, the same amount of deformation will be uniformly distributed in more grains. The length and number of dislocation clusters within the grains will be reduced, which effectively reduces the stress concentration and improves the ductility of the material [133]. In addition, the inhibition of dislocation motion achieves an effective improvement in mechanical properties.

Grain size also has an important effect on the phase transition temperature and damping properties. In general, as the average grain size decreases, the nucleation rate of austenite increases, which will promote the reverse MT. At the same time, the martensitic phase transition temperature moves to a lower temperature. The former is due to the stabilizing effect of grain boundaries on austenite, while the latter is due to the fact that both the martensite/martensite interface and grain boundaries are preferred locations for austenite nucleation [117].

The strong sensitivity of the phase change temperature to grain size provides us with a relatively simple way to control the phase change temperature [113]. At the same time, grain refinement has a double-sided effect on the damping capacity of the alloy [93,131]. On the one hand, grain refinement can reduce the interlayer spacing of martensite, which increases the number of interfaces per unit volume and facilitates the improvement of damping performance; on the other hand, with the excessive reduction of interlayer spacing, the compressive stress at adjacent interfaces and the bonding force at grain boundaries increase, leading to a decrease in the interfacial slip and a decrease in damping performance. Therefore, adjusting the composition of the alloy is an effective way to improve the mechanical properties and damping properties of the alloy.

4.2 The effect of heat treatment

Heat treatment is one of the most important processes in mechanical manufacturing. It improves the performance of the workpiece by changing the internal microstructure or the chemical composition of the surface [134,135]. In practical application, in order to improve the mechanical

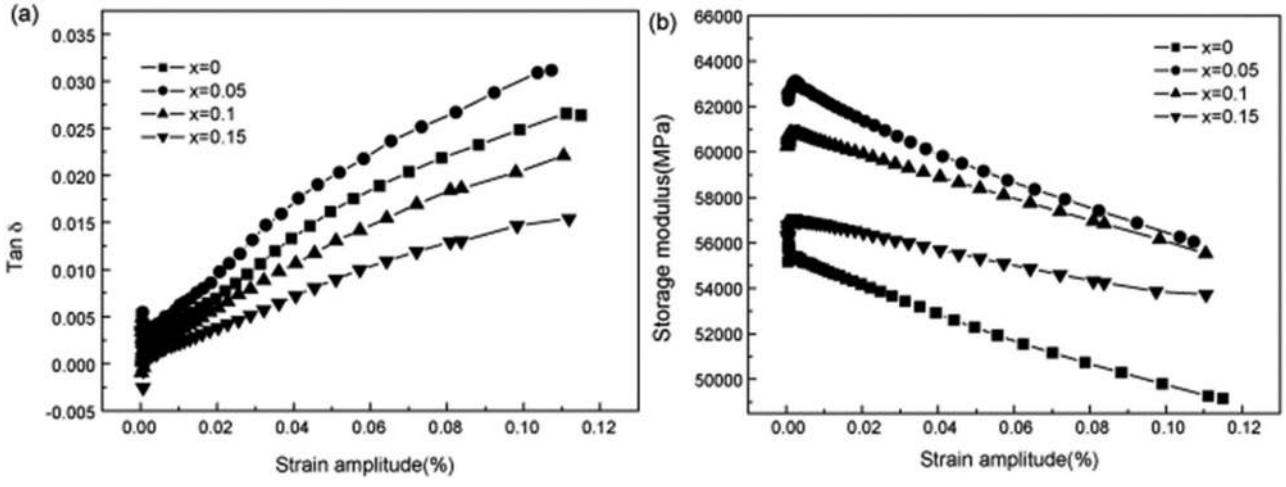

Figure 9: Damping characterization of Cu–12Al–5Mn alloys with different Ce contents: (a) the variation trend of tan δ with strain amplitude and (b) the variation trend of storage modulus with strain amplitude [86].

properties of metal materials, heat treatment technology is often essential besides the rational selection of materials and processing technology.

Many properties of Cu-based alloys are related to their thermoelastic MT, which is very sensitive to the heat treatment process [123]. In order to obtain a full martensite structure, Cu-based alloys are usually treated by solution treatment and aging treatment. The solid solution treatment is to heat the alloy to the high-temperature β-single-phase region and quench it after holding at a specified temperature and time to obtain the supersaturated solid solution, namely the martensite structure [136]. The excessive cooling rate in the quenching process is easy to cause incomplete ordering and the formation of many vacancies and dislocations [127]. Therefore, after solution treatment, aging treatment is usually adopted to eliminate unwanted defects and stabilize the phase transition point of the alloy [137]. Cu-based alloy aging in the martensitic state and parent phase will produce different effects. In general, aging in the martensitic state causes martensitic stabilization problems [137]. Finally, the inverse martensitic temperature of the alloy will increase, and more seriously, the reverse MT will be completely suppressed, which is harmful to the damping performance of the alloy. Aging in the parent-phase state can realize the reordering of alloy and reduce the number of vacancy defects [138]. However, appropriate process parameters should be selected for the aging of the parent phase. Because the quenched sample is a supersaturated solid solution, extremely high aging temperature or long time will cause the equilibrium phase precipitation of the alloy [136]. Therefore, after proper solution and aging treatment, not only the damping performance can be improved by regulating the behavior of thermoelastic martensite, but also the dislocation and grain boundary movement can be impeded through the generation of the second phase to improve the strength [139].

4.2.1 The effect of heat treatment on the microstructure

The unique microstructure of Cu-based alloys, such as grain size, martensite type, and the presence of second-phase particles, provide excellent mechanical properties and high damping performances [140,141]. These microstructures are largely affected by the heat treatment process. When the alloy is heated to the high-temperature β-phase region for solution treatment, the increase of temperature and entropy will promote grain growth. When the grains grow, there will be a large slip on the grain boundary during the deformation process, and then the stress concentration will be generated at the grain boundary to maintain the coordination between the grain boundaries. When these stress concentrations accumulate gradually and reach the bearing limit of grain boundary, cracks will occur at the grain boundary and lead to fracture. For the sake of reducing negative effects, researchers have carried out a lot of studies on the heat treatment process.

Ren *et al.* [142] obtained Cu–Al alloys with different size grains by controlling the heat treatment temperature, as shown in Figure 10. It is found that the grain size of the alloy increases with the increase of temperature, especially from 600 to 800°C. Dalvand *et al.* [143] studied the effect of isothermal aging on the microstructure of

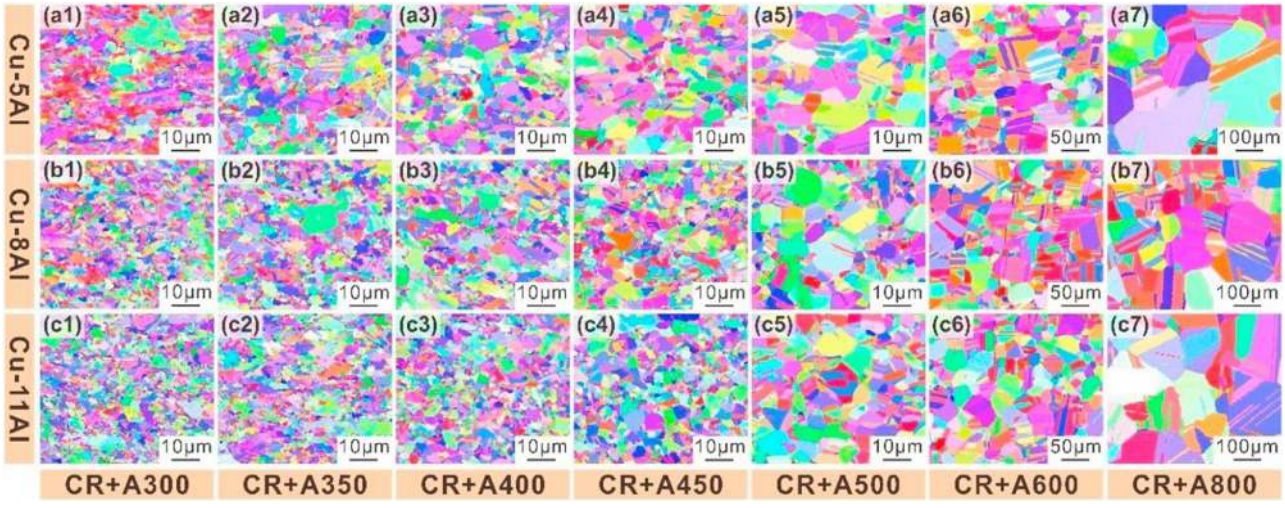

Figure 10: The microstructure of Cu–Al alloy at different annealing temperatures increases from left to right: (a1–7) Cu–5Al alloys, (b1–7) Cu–8Al alloys, and (c1–7) Cu–11Al alloys [142].

Cu–12Al–3.5Ni–0.7Ti–0.05RE (RE = Ce, La) alloy, and found that the effect of aging at 250°C was small, but the long aging at 350°C led to the decomposition of the parent phase into equilibrium γ_2 and α phases. Qader *et al.* [123] studied the microstructure evolution of Cu–13Al–3Ni–4Hf during aging and found that β-phase (Cu_3Al) would be generated after aging above 973 K, which would change the microstructure of the alloy. Suresh *et al.* [140] conducted aging treatment on Cu–13.4Al–4Ni alloy at 473–573 K and found that γ_2 precipitates appeared at 473 K and the volume fraction of γ_2 precipitates increased with the increase of aging temperature. Yildiz [144] observed the microstructure of Cu–Al–Ti–Ta alloys at different cooling rates. The results showed that water cooling and air cooling mainly produce a large amount of 18R and a small amount of 2H martensite, and furnace cooling produced a sharp increase in the amount of 2H martensite. Wang *et al.* [145] treated the Cu–11.9Al–2.5Mn alloy with different cooling methods and showed that all samples except furnace cooling clearly showed lath martensite and twin structures. The excessively fast cooling rate would also increase the dislocation density and provide a heterogeneous nucleation location for martensite formation [22]. In short, through the control of the heat treatment process (temperature, holding time, cooling rate, *etc.*), the comprehensive performance can be improved by adjusting the microstructure.

4.2.2 The effect of heat treatment on mechanical properties

Mechanical properties are the basic properties of materials, which ultimately determine the bearing capacity, service life, and safety of structures. Due to the large anisotropy and grain size of Cu–Al alloy, brittle fracture, and low fatigue strength will reduce its mechanical properties and service life [123]. Therefore, how to improve the mechanical properties of Cu-based alloys has become the focus of many researchers.

Ren *et al.* [142] conducted heat treatment of Cu–Al alloy at different temperatures, and the results showed that with the increase of temperature, the grain was refined and the hardness and strength were improved, as shown in Figure 11. Qader *et al.* [123] studied the change in mechanical properties of Cu–13Al–3Ni-4Hf during aging and found that β-phase (Cu_3Al) would be generated after aging above 973 K, which would increase the brittleness of the alloy. In other studies, it was also confirmed that the increase of the α phase would lead to the increase of thermal stability and the decrease of the hardness of the alloy [146]. Saud [146] also showed that aging treatment improved the ductility of Cu–Al–Ni alloy. In addition, mechanical failure of Cu-based alloys was also related to brittle intergranular fracture caused by high shear stress concentration at grain boundaries [24]. High shear stress concentration occurs due to high elastic anisotropy and incompatible deformation of adjacent grains, as shown in Figure 12(a) [147]. At an appropriate cooling rate, the Cu-based alloy consists of two layers of columnar grains. A single layer of columnar grains will form at a cooling rate that is high enough, as shown in Figure 12(b). Monolayer structures reduce the number of potential crack initiation sites and shear stress concentration caused by elastic anisotropy. Therefore, in order to obtain excellent mechanical properties, the selection of appropriate heat treatment process parameters can achieve the purpose.

4.2.3 The effect of heat treatment on martensite transformation

The MT mechanism of Cu-based alloys is usually related to the change in structure/properties during heat treatment [22,81]. Both the solution treatment time and the holding temperature can affect the phase transition temperature. The longer the solution time or higher the holding temperature will increase the phase transition temperature. It is mainly affected by the size of the crystal grains; the larger the crystal grains, the higher the phase transition temperature. However, defects such as vacancy and dislocation will be formed during the process of solid solution and quenching. The pinning effect of vacancies and dislocations on the interface could also increase the reverse MT temperature of the alloy [145]. In the long-range ordered parent phase, the diffusion of atoms through vacancy migration pointed to energy-favorable routes [148]. However, this was not the case in the martensitic structure. The migration of vacancies near the martensite interface did not occur sufficiently, resulting in the retention of disordered atomic pairs or locally disordered structures in the martensite. Thus, excessive vacancies were gathered around dislocation and martensite interface, resulting in martensite stability [144]. The increase of martensite stability is baleful to the phase transformation of the alloy. The kinetics of the phase transformation is reflected in the Kissinger and Flynn–Wall–Ozawa models [149].

The Kissinger model is given by equation (10) [150]:

$$\frac{\mathrm{d}\ln(\beta/T_p^2)}{\mathrm{d}\ln(1{,}000/T_p)} = -E_a/R, \tag{10}$$

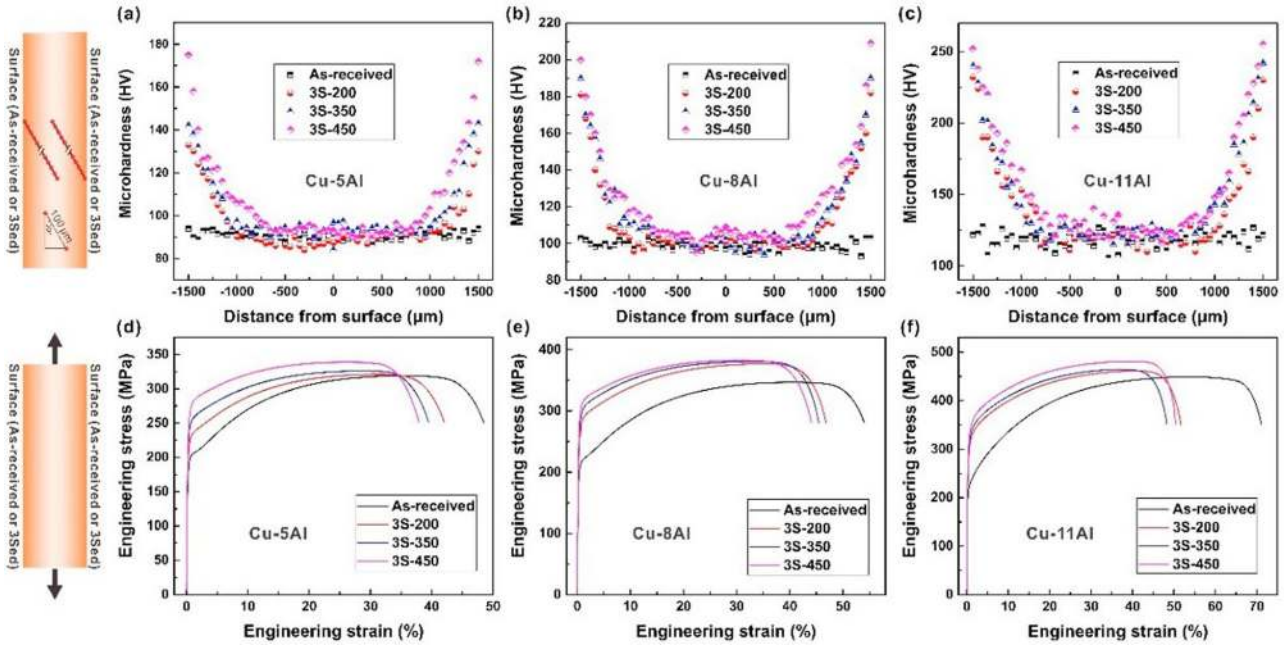

Figure 11: Microhardness and tensile strength curves of the Cu–Al alloy annealed at 400, 450, and 500°C: (a–c) microhardness and (d–f) tensile strength [142].

where β is the heating/cooling rate; T_p is the temperature of maximum intensity of the reaction; E_a is the activation energy; and R is a constant.

The Ozawa model is given by equation (11) [151]:

$$\ln(\beta) = \text{const}(10{,}518 \times E_a/RT_p). \tag{11}$$

Meanwhile, the relaxation energy during MT can be expressed as equations (12–14) [145]:

$$E_d = \Delta S\left(\frac{A_f - M_s}{2}\right), \tag{12}$$

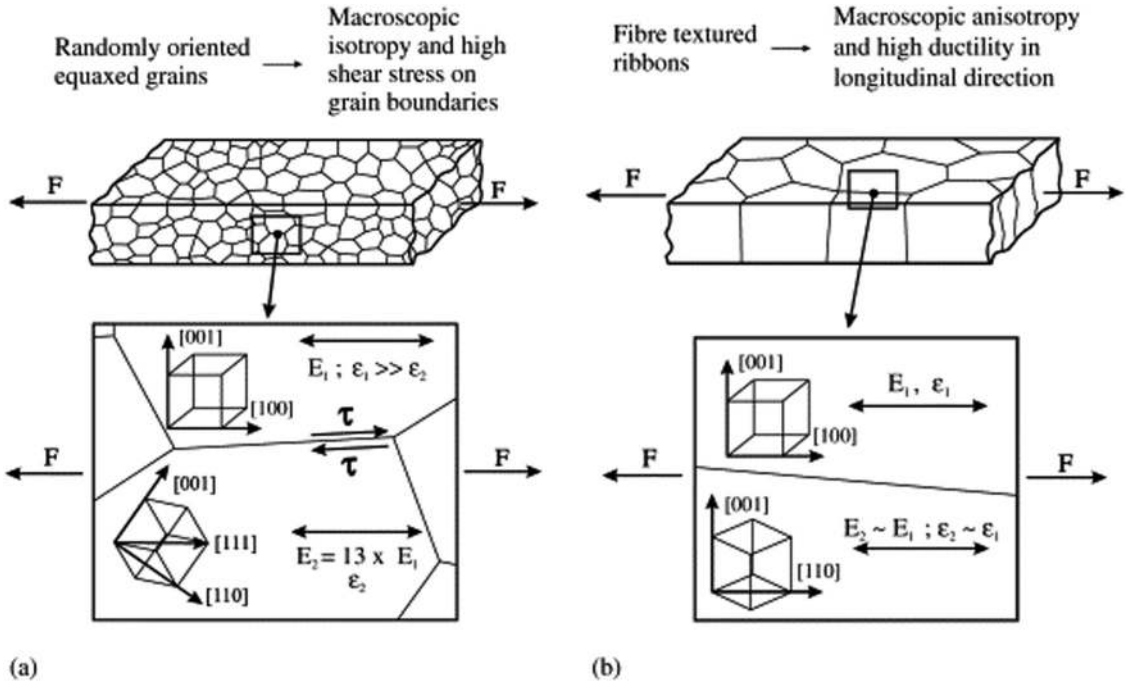

Figure 12: (a) Multilayer equiaxed structure and (b) single-layer columnar fibre textured structure [147].

$$\Delta S = \frac{\Delta H}{T_o}, \tag{13}$$

$$T_o = \frac{M_s + A_f}{2}, \tag{14}$$

where ΔS is the change in entropy during MT; ΔH is the enthalpy change during reverse MT; and T_0 is the thermodynamic equilibrium temperature where the Gibbs free energy is equal to zero.

Undesired structural defects in the alloy (such as quenching stress, quenching vacancy, *etc.*) can be eliminated by aging, which is usually the process that determines the final physical properties [20]. Therefore, the relationship between heat treatment and MT has been extensively studied in recent years [130]. After Cu–13Al–4Ni–4Fe is heat-treated at 950°C, the increase of the thickness and grain size of martensite lath relaxes the microstrain, leading to an increase in the phase transition temperature of the alloy [152]. Wang *et al.* [137] studied the effect of aging on porous CuAlMn alloy and found that after aging at 350°C, due to the refinement of the martensitic structure and the elimination of quenching vacancies, the damping capacity of martensitic alloy and the height of the internal friction peak caused by reverse MT increased. In addition, the cooling medium also plays an important role in the process of solid solution and aging because different cooling media determine different cooling rates [22]. Generally, the cooling rate can be determined by the ratio of ΔT and Δt, where ΔT is the change in the quenching temperature and Δt is the time cost during the cooling process. Yildiz [144] studied the effect of different cooling rates on the phase transition temperature of the alloy. Water cooling was a one-step transformation in both MT and reverse MT processes, while air cooling and furnace cooling were characterized by a two-step transition. Studies have shown that the reduction of the cooling rate will move the phase transition temperature to high temperatures, and the effect of the heat treatment temperature on the change of the phase transition temperature and enthalpy is different, as shown in Figure 13 [123]. Therefore, the temperature and cooling rate during heat treatment have important effects on the phase transformation behavior of the alloy.

4.2.4 The effect of heat treatment on damping performances

The damping capacity of Cu-based alloys comes from the inelastic strain of the phase interface and martensite twin boundary [140]. These interfaces can move continuously under alternating external stresses, thereby releasing stress and consuming mechanical energy. There were two peaks in the damping of Cu-based alloy, the high-temperature phase was due to anti-martensitic phase transformation, and the low-temperature phase was due to pseudo-first-order phase transformation during twinning thinning [145]. The density and distribution of inherent structural defects (vacancies, dislocations, grain boundaries, and precipitates) of the martensite phase-controlled the overall damping peaks of these alloys [140].

The damping peaks of low-temperature twins play an important role in the damping mechanism of Cu-based alloys. According to Zhang and Liu [112], when the twins were relatively rough or the space between the twin walls was relatively large, the twins were very likely to move due to the relatively weak interaction between the twin walls. However, if the space was small enough, the elastic

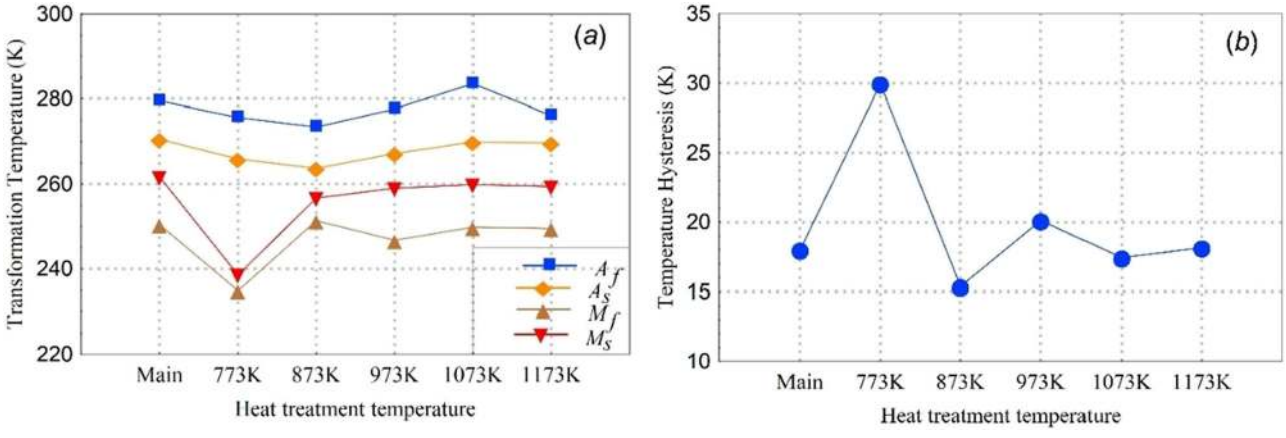

Figure 13: (a) Phase transition temperature of Cu–13Al–3Ni–4Hf alloy at different temperatures and (b) temperature hysteresis for each case [123].

strains caused by the twin walls would overlap, making the movement of adjacent twin walls difficult, resulting in reduced damping. The high-temperature damping peak is very sensitive to temperature [114]. Thermoelastic martensitic stability could be obtained by tempering the quenching alloy below the As for a long time. This led to a decrease in the thermoelastic behavior of martensite, which greatly reduced the damping performances of the material [151,153]. For quenched samples, the quenching vacancies were highly concentrated and randomly distributed [136]. When aging starts in the martensite phase, the vacancy will gradually accumulate toward the dislocation or interface, impeding the migration of dislocation and interface, and reducing the internal friction related to dislocation and interface movement [152]. In addition, the reverse MT will also be hindered, leading to an increase in the MT temperature and a decrease in the peak strength of phase change damping caused by the reverse MT [149].

In consequence, researchers have done a lot of work on the relationship between temperature and damping. Studies showed that as the ambient temperature increased, the damping increased at first. This was mainly because though the amount of martensite was reduced, more phase interfaces and twin boundaries could move at a higher temperature, resulting in higher energy consumption. When the ambient temperature was higher than M_s, with the further increase of the ambient temperature, the damping performances decreased sharply, mainly because there was little martensite remaining in the alloy [154]. Wang *et al.* [138] studied the effect of aging treatment on Cu–11.7Al–2.49Mn alloy and found that with the increase of aging temperature, the strength of the internal friction peak began to increase, and then the reverse martensite transformation decreased, as shown in Figure 14. In addition, the shift of the peak position from low temperature to high temperature was attributed to the thinning of martensite lath and the disappearance of quenching vacancy. Li *et al.* [136] studied the effect of aging treatment at 250–400°C on the damping properties of columnar Cu–Al–Mn shape memory alloys and their mechanism. The results showed that the maximum damping peak is 0.11. With the increase of aging temperature and time, the precipitates of bainite increased but the damping capacity of columnar Cu–Al–Mn shape memory alloy decreased at first, then increased, and finally decreased again. The more complete the MT is, the more energy is consumed, which increased the inherent damping of the alloy [20]. In addition, intermetallic precipitated particles formed in the aging process have a pinning effect on martensite variants, which will reduce the damping capacity [136,152]. Therefore, in the choice of heat treatment, only the appropriate heat treatment process can achieve the ideal effect.

4.2.5 Summary of heat treatment mechanisms

The unique martensitic structure of Cu–Al-based alloys determines that the heat treatment process plays an important role in its mechanical and damping properties. The solid solution treatment is mainly to obtain a supersaturated solid solution. The aging treatment is to eliminate the defects such as vacancies formed in the solid solution treatment. In the process of heat treatment, the grain size can be adjusted through reasonable control of the process parameters, and then the mechanical

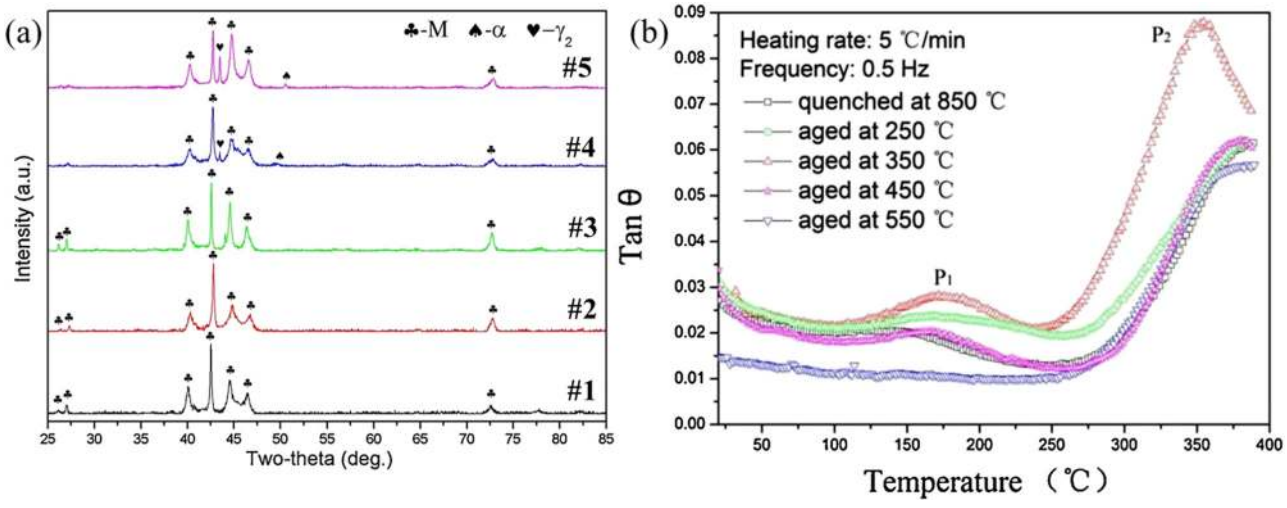

Figure 14: Cu–Al–Mn alloy treated at different temperatures: (a) XRD patterns and (b) the damping properties [138].

properties of the alloy can be improved through the fine grain strengthening effect. Structural defects in martensite have a significant impact on damping properties. The ultimate purpose of both solid solution and aging treatments is to improve the damping performance by modulating the energy-consuming movable interfaces and defects. The two-sided effect of grain refinement on damping properties was also mentioned earlier so a proper choice of the heat treatment process is also needed to achieve the ultimate improvement.

4.3 The combination of alloying and heat treatment

In order to fully take advantage of both alloying and heat treatment, the combined application of the two must be discussed. Saud *et al.* [155] found that the highest internal consumption value shown by the Cu–Al–Ni alloy after the addition of 3 wt% Ta element was closely related to the solid solution of this alloy after 30 min at 900°C. The substable phase generated by rapid cooling after solid solution facilitates the occurrence of martensitic phase transformation and further improves the damping properties of the alloy. The mechanical properties of the alloy are influenced by the pore-density, grain refinement, and precipitates. These parameters affect the mechanical properties by controlling the dislocations and the motion of the martensitic interface [155]. Mallik and Sampath [18] mentioned that the damping capacity of Cu–Al–Mn-based alloys increases with increasing Al content when the Mn content was constant. When the Al content was constant, the damping capacity of the alloy decreased with increasing Mn content. The alloys with different Al and Mn contents were also subjected to isothermal aging after quenching in the austenitic phase at 300°C and 500°C for 2 h. It was found that the γ_2 phase generated after aging at 300°C would reduce the Al content in the base material and thus increase the phase transformation temperature; 500°C aging would produce more γ_2 phase and further reduce the Al content in the base material. The phase transformation of martensite is finally suppressed by changing the Al content and the inhibiting effect of precipitation on interfacial mobility. Milhorato and Mazzer [156] in their study of Cu–11.35Al–3.2Ni–3Mn alloy found that trace amounts of Nb elements will increase the hardness. Aging treatments in the temperature range of 300–550°C revealed the formation of new phases in the interfacial region, within the grain boundaries and between the martensitic variants as the temperature increased. The compressive strength was up to 1,400 MPa when the temperature was 500°C. Li *et al.* [157] systematically investigated the effects of parent-phase aging and Nb elements on the comprehensive properties of Cu–Al–Mn-based alloys. It was found that parent-phase aging can effectively improve the low-temperature damping and damping peak of the alloy due to the increase of interfacial mobility. The best damping was obtained at 600°C aging. The effect of the addition of Nb content on the damping properties of the alloy after aging at 600°C was also investigated. It was found that the $AlNb_3$ generated by the addition of Nb content could significantly refine the grains and the maximum value of damping occurred at Cu–Al–Mn–0.7Nb.

Therefore, an effective combination of heat treatment and alloying can achieve further improvement of alloy properties. Alloying can improve the mechanical and damping properties by controlling the grain size to achieve fine-grained strengthening and provide more movable interfaces for energy consumption. Usually, solid solution treatment along with alloying will promote the formation of martensite, which is beneficial to the damping properties of the alloy. However, the presence of many vacancies after solution quenching can also have a pinning effect on the martensite interface, which in turn increases the anti-martensite phase transition temperature and inhibits the martensite phase transition. The effective aging treatment after quenching can reduce or even eliminate the adverse effects of quenched vacancies. Therefore, if the combination of alloying, solution treatment, and aging treatment can be achieved, it is beneficial to obtain Cu–Al-based alloy with better comprehensive performance.

5 Nanoreinforcement

At present, other than alloying and heat treatment that play an important role in improving the comprehensive performance of alloys, nanotechnology is also gradually receiving more attention from researchers. Nanomaterials show higher strength and diffusivity due to their unique nanoscale structure, so the use of nanoreinforcement is considered an effective method to obtain high-performance alloys [158]. Materials typically smaller than 100 nm in size play a major role in the pinning of dislocations, are often used as enhancers for metal property improvement, and show their full potential in terms of mechanical and functional properties [159,160]. The improvement of these properties is closely related to the characteristics of matrix and reinforcement particles, the bonding between the reinforcement and matrix, and the size and distribution of the

reinforcement in the matrix [161]. Also, the simultaneous strengthening of grain boundary reinforcement and nanoparticles is promising to obtain better microstructure and comprehensive properties.

5.1 Effect of nanoreinforcement on mechanical properties

Studies have reported that Al_2O_3, ZrO_2, and Y_2O_3, as nano-reinforcing phases, have shown impressive ability to improve the mechanical properties and functional properties of metal-based materials [159,160,162]. This is mainly due to the increased proportion of finer grains, solid solution strengthening, and dispersion strengthening. Abbass and Sultan [163] showed that nanoparticles can improve the hardness of alloys by reducing the porosity of the material, thus improving the microstructure of the alloy. The increase in hardness is also closely related to the high hardness of the nanoparticles. Lee *et al.* [164] prepared Cu–Al-based alloy with nano-Al_2O_3 dispersion distribution by hot extrusion process and found that the yield strength and tensile strength would increase with the increase of the Al_2O_3 volume fraction. Yang *et al.* [165] found that the addition of dispersed Y_2O_3 nanoparticles to titanium alloys improved strength and ductility. Kumar *et al.* [159] showed that the addition of nano-Y_2O_3 reinforcements to Mg–3Al–2.5La alloys significantly reduced the grain size to 3.6 μm (only 43% of the matrix), improving the strength. These nanoenhanced phases will increase the strength by inhibiting the motion of dislocations. In addition to the pegging effect, they can also act as forming nucleation spots during solidification and recrystallization, further reducing the grain size [159]. These nanoparticles mainly hinder dislocations and interfacial slip to increase mechanical properties, which is the Orowan strengthening mechanism shown in equations (15) and (16) [165]:

$$\Delta\sigma_{\text{Orowan}} = \frac{0.13Gmb}{\lambda}\ln\left(\frac{d}{2b}\right), \tag{15}$$

$$\lambda = d\left[\left(\frac{1}{2V}\right)^{1/3} - 1\right], \tag{16}$$

$\Delta\sigma_{\text{Orowan}}$ is the increment of YS caused by the Orovan strengthening mechanism; Gm is the shear modulus of the matrix; b is the Burgers vector of the matrix; d is the particle diameter; and λ is the interparticle spacing.

In addition to the mentioned nanoreinforced phases, graphene and CNTs have shown favorable reinforcement in metal-based materials and are also of wide concern. CNTs are one of the most attractive reinforcing materials due to their high thermal conductivity, low thermal expansion coefficient, high damping ability, and proper self-lubricating behavior [166,167]. The distribution scale of CNTs is much finer than that of ordinary fibers, which prevents crack extension and the generation of microcracks. Chen *et al.* [168] showed that the addition of graphene significantly enhanced the mechanical properties of Cu alloys. Shu *et al.* [65] exploited the synergistic enhancement of graphene and CNTs, which significantly improved the mechanical properties of Cu-based alloys mainly through the generated high-density dislocations, grain refinement, and load transfer effects [168]. Among several strengthening mechanisms of graphene, dislocation strengthening plays a very important role, as shown in Figure 15. Figure 15(a) shows the multilayer and impenetrable graphene layer structure with which it restricts the movement of dislocations and effectively improves the strength of the alloy. Figure 15(b) shows the variation of dislocations and interfaces. When the dislocations slip into the graphene interface, steps are formed under the interface, leading to the concentration of interfacial stress. Therefore, the motion of dislocations is hindered by large stress, and the strengthening effect is achieved.

5.2 Effect of nanoreinforcement on damping properties

In addition to the improvement of mechanical properties, these nanoparticles have achieved satisfactory results in terms of improvement of damping properties. The damping enhancement exerted by nanomaterials is mainly due to the energy consumption through interfacial sliding and friction between the matrix and the reinforcing phase [169,170]. In addition, the presence of high dislocation density around the reinforcement is another possible factor for the increased damping capacity [158,170]. Srikanth *et al.* [171] found that the presence of nano-Al_2O_3 increases both the hardness and damping capacity of pure Mg alloys. The increase in damping is closely related to the various microstructural changes induced by the nanoreinforced phase. The difference in thermal expansion coefficients between the matrix and the nanoreinforced particles promotes the occurrence of dislocation damping mechanisms. When the dislocation is pinned by impurity atoms, it plays the role of an elastic vibrating string to increase energy consumption. In conclusion, the presence of damping sources is closely related to the microstructure [158]. For metallic materials,

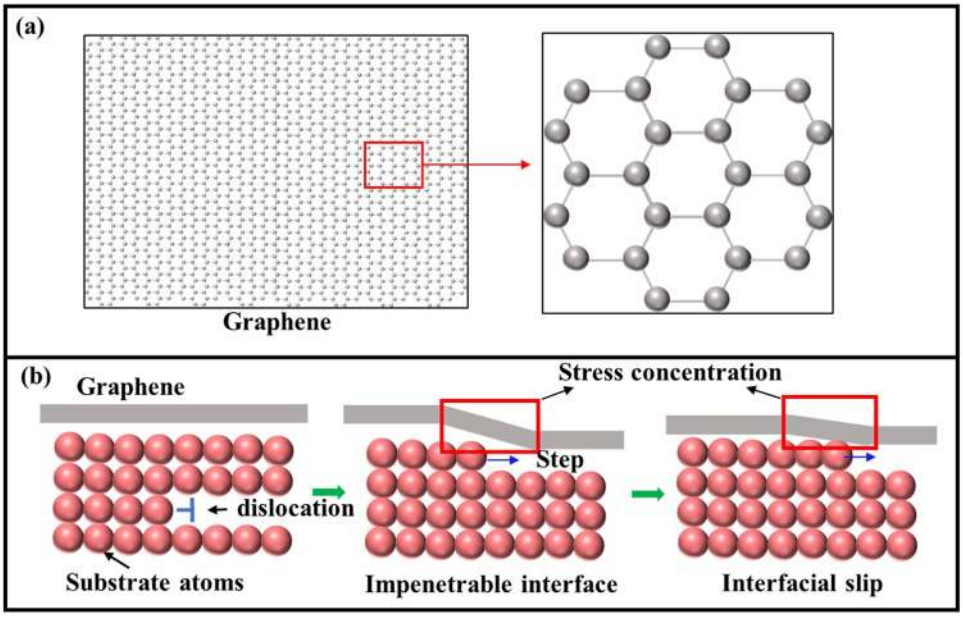

Figure 15: (a) The honeycomb lattice arrangement of graphene (b) the interaction between dislocation and interface.

different forms of damping sources coexist, such as point defects, dislocation motion, grain boundary slippage, and friction between the second phase and the substrate. Nanoparticles have more interfacial defects, such as triple boundaries and elastic deformation layers. Meanwhile, Severson *et al.* [172] developed a particle dynamics simulation model to investigate the effect of nanoparticles on the damping properties of the alloy. The simulation results again proved that nanoparticles can be used as a novel damping medium to dissipate energy through viscous hysteresis. This is because they dissipate energy through friction when flowing and impacting due to viscoelastic or plastic deformation between particles.

The influence of CNTs and graphene in enhancing damping cannot be underestimated. CNTs show great potential in damping performance, mainly in the following aspects [173]. (1) Viscoelastic energy dissipation of CNTs. It has a significant Young's modulus and deformability, exhibiting high damping capacity [174]. (2) Due to the addition of CNTs, multiphase interfaces and various forms of interfaces are created, which then generate large interfacial friction and slip during vibration [175]. (3) Interphase damping in the region of the surface between nearby CNTs [176]. Carvalho *et al.* [170] showed that by reinforcing AlSi-SiCp with CNTs, the damping capacity was improved without reducing the mechanical properties. Ebrahimi *et al.* [166] found that the addition of CNTs can regularly increase the high-temperature damping behavior compared to the matrix AZ91D alloy. Compared with CNTs, graphene has a 2D sheet structure and is also an attractive damping reinforcement material. With graphene as a reinforcing phase, its damping enhancement mechanism mainly comes from the following aspects [177]: (1) the difference in thermal expansion coefficients between graphene and the substrate material increases the dislocation density at the interface between them; (2) under the effect of alternating stress, the higher elastic modulus of graphene facilitates the conversion of vibrational energy into thermal energy consumption; and (3) the weaker interface between graphene and the substrate and also alternating stresses will consume energy by generating friction. The superiority of CNTs and graphene has led to their wide application as a reinforcing phase in recent years.

It is noteworthy that nanoreinforced phases have made great achievements in improving the mechanical and damping properties of other metals. However, it is rather lacking in the study of Cu–Al-based alloys. Therefore, this article provides ideas for the development of nanoreinforced phases in Cu–Al-based alloys.

6 Conclusions

Cu–Al-based alloys have been widely used in the field of damping in recent years. In this article, the effects of alloying and heat treatment on the mechanical and damping properties of Cu–Al-based alloys are reviewed. Meanwhile, the advantages of nanoreinforced alloys in

terms of mechanical and damping properties are briefly introduced, and the feasibility of adding nanoreinforced phases to Cu–Al-based alloys to improve damping properties is proposed. The conclusions are as follows:

(1) With respect to material preparation, Cu–Al-based alloys with high density, uniform element distribution, and ideal comprehensive properties can be obtained by combining mechanical alloying and powder metallurgy.
(2) Rational control of grain size is the key to obtain high mechanical properties and high damping performances of Cu–Al-based alloys. When the grain size is larger, it is easy to cause a brittle fracture and reduce the mechanical properties. Moreover, a large grain size will reduce the interface damping effect, which is harmful to obtaining high damping performances.
(3) The insolubility of alloying elements and their reaction with parent elements to form fine compounds will hinder the growth of grain, which are beneficial to reduce the grain size, change the microstructure, and improve the comprehensive properties. In addition to alloying elements, inoculants can refine grains through heterogeneous nucleation and grain boundary refinement. An appropriate combination of the two can further control the grain size of the alloy. During the selection of inoculant, the wettability and lattice matching degree between matrix and inoculant are crucial.
(4) Adopting appropriate solution heat treatment and aging heat treatment can obtain materials with ideal properties. The process mainly affects the phase transition temperature and the difficulty of phase transition by changing the grain size, phase composition, and the existence of the second phase particles. Eventually, the mechanical properties and damping performances of the alloy are improved.
(5) The close combination of the addition of alloying elements and the heat treatment processes can further improve the comprehensive properties of the alloy through the increase of fine grain strengthening and damping interface effect. It provides an idea for the synthesis of Cu–Al-based materials with high strength and high damping.
(6) Nanomaterials not only have the advantages of high hardness and strength due to their unique nanosize structure but also have been widely used as a reinforcing phase to improve the mechanical properties and damping characteristics of metal materials. The improvement of mechanical properties is mainly achieved by the pinning of dislocation and the obstruction of interface movement by uniform fine nanoparticles. The damping performance is improved mainly by the interface friction between the matrix and the reinforcing phase and the high-density dislocation around the reinforcing phase.

7 Future perspectives

Cu–Al-based alloy has good comprehensive properties and application prospects by virtue of its unique characteristics and thermoelastic martensite structure. Based on the literature research, the future development of Cu–Al alloy is also considered and prospected. In order to promote the development of the materials industry, materials are no longer only sufficient to meet the unilateral excellent performance but often need a comprehensive performance. There are many factors that affect the performance of a particular aspect of material and each factor requires a lot of experiments to verify, which is a complex and time-consuming process. Fortunately, the computer industry has realized rapid developments in the field of materials with the gradual optimization and improvement of big data. Thus, in addition to alloying, heat treatment, and nanoreinforcement, numerical simulations, and 3D printing techniques are proving to have great potential. They reduce the influence of human errors and laboratory variables, and now the field of materials has become a research focus for researchers [178,179].

7.1 Numerical simulation

With the gradual optimization and improvement of numerical simulation theory, it has been favored by many researchers. It can make the operation more effective to predict the microstructural changes based on the changes in experimental parameters, which helps to reduce the defects in materials [180,181]. Meanwhile, the results of numerical simulations can clearly reflect the experimental testing process, highlighting its realism and reliability. Tsai and Hwang [180] used the finite difference method to obtain the macroscopic temperature and microscopic concentration fields to effectively predict the microstructural morphology of Cu–0.6Cr alloys prepared by the vacuum continuous casting process. Therefore, in order to improve the comprehensive performance and achieve a more effective study, computer simulations can be used to analyze the effects of different parameters on the mechanical and damping properties of Cu–Al-based alloys. This technique usually requires a

complete and prepared simulation model in order to simulate a real working environment. The presence of defects can be detected and eliminated by changing the key operational parameters during numerical simulations, providing theoretical guidance for the design of parameters for experiments [182]. Currently, computer technology is playing an increasingly important role in the design and preparation of metal alloys, which can contribute to its further development [183]. Its interdisciplinary development is also an important direction to obtain high-performance materials, and it is an inevitable trend to achieve the integration of functionalization and intelligence.

7.2 3D Printing technology

3D printing technology is a manufacturing process for constructing free-form shapes and structures based on computer-aided design models. With its ability to build complex shapes and save raw materials, it has successfully produced a variety of materials with different properties (including polymers, composites, metals, and ceramics) [184–186]. Selective laser melting (SLM) is a commonly used 3D printing technique that focuses on the use of the principle of laser irradiation sintering to form metal powders or nonmetal powder stacks under the control of a computer program. It can increase the laser power and accurately melt the metal powder layer to directly print metal parts [187–189]. Currently, it has been widely used for titanium alloys. Kacenka *et al.* [190] successfully compared the difference of electrochemical hydrogenation between 3D printing (SLM) and forging Ti–6Al–4V alloys under the same parameters, providing guidance for the mechanism of hydrogen action in 3D printing Ti–6Al–4V alloys. In addition, 3D printing technology was used to improve the properties of Co–Cr alloy, and it was found that SLM technology had a positive effect on the mechanical properties and electrochemical properties [189]. Also, due to the controllable laser power of the SLM technique, the prepared metals usually have an ultrafine grain structure, and the excellent microstructure obtained has a positive influence on the hardness, strength, and elastic modulus of the material [179,184].

With many achievements in metal materials, 3D printing technology has now become an indispensable complement to traditional mechanical engineering. The superiority of this technology in other fields has also provided researchers with certain ideas and guidance for the future development in the field of Cu–Al-based alloys. However, in the field of Cu–Al-based alloys, there is a lack of research and application of this technology. Therefore, if the superiority of 3D printing technology can be fully utilized in the field of Cu–Al-based alloys, it is expected that more efficient preparation of desirable materials can be achieved.

Funding information: This work was supported by Key Laboratory of Infrared Imaging Materials and Detectors, Shanghai Institute of Technical Physics, Chinese Academy of Sciences (No. IIMDKFJJ-19-08), and China Postdoctoral Science Foundation (No. 2015M570794, No. 2018T110993).

Author contributions: All authors have accepted responsibility for the entire content of this manuscript and approved its submission.

Conflict of interest: The authors state no conflict of interest.

References

[1] Sun L, Huang WM, Ding Z, Zhao Y, Wang CC, Purnawali H, et al. Stimulus-responsive shape memory materials: a review. Mater Des. 2012;33:577–640. doi: 10.1016/j.matdes.2011.04.065.

[2] Sutou Y, Omori T, Wang JJ, Kainuma R, Ishida K. Characteristics of Cu-Al-Mn-based shape memory alloys and their applications. Mater Sci Eng A. 2004;378(1–2):278–82. doi: 10.1016/j.msea.2003.12.048.

[3] Oliveira JP, Zeng Z, Omori T, Zhou N, Miranda RM, Braz Fernandes FM. Improvement of damping properties in laser processed superelastic Cu-Al-Mn shape memory alloys. Mater Des. 2016;98:280–4. doi: 10.1016/j.matdes.2016.03.032.

[4] Tian QC, Yin FX, Sakaguchi T, Nagai K. Reverse transformation behavior of a prestrained MnCu alloy. Acta Mater. 2006;54(7):1805–13. doi: 10.1016/j.actamat.2005.12.007.

[5] Alaneme KK, Umar S. Mechanical behaviour and damping properties of Ni modified Cu-Zn-Al shape memory alloys. J Sci. 2018;3(3):371–9. doi: 10.1016/j.jsamd.2018.05.002.

[6] Chen KW, Yan JZ, Li N, Luo ML, Shi HJ, Zhu X, et al. The effect of the annealing temperature on the damping capacity under constant prestress, mechanical properties and microstructure of an Fe-11Cr-2.5Mo-0.1Zr-1.0Ni forged damping alloy. J Alloy Compd. 2020;815:152429. doi: 10.1016/j.jallcom.2019.152429.

[7] Liu XJ, Wang QZ, Kondrat'ev SK, Ji PG, Yin FX, Cui CX, et al. Microstructural, mechanical, and damping properties of a Cu-based shape memory alloy refined by an in situ LaB6/Al inoculant. Metall Mater Trans A. 2019;50:2310–21. doi: 10.1007/s11661-019-05153-9.

[8] Shivasiddaramaiah AG, Mallik US, Shivaramu L, Prashantha S. Evaluation of shape memory effect and

damping characteristics of Cu-Al-Be-Mn shape memory alloys. Perspect Sci. 2016;8:244–6. doi: 10.1016/j.pisc.2016.04.041.
[9] Karagoz Z, Canbay CA. Relationship between transformation temperatures and alloying elements in Cu-Al-Ni shape memory alloys. J Therm Anal Calorim. 2013;114(3):1069–74. doi: 10.1007/s10973-013-3145-9.
[10] Laper ML, Guimaraes R, Barrioni BR, Silva PAP, Houmard M, Mazzer EM, et al. Fabrication of porous samples from a high-temperature Cu-Al-Ni-Mn-Nb shape memory alloy by freeze-drying and partial sintering. J Mater Res Technol-JMRT. 2020;9(3):3676–85. doi: 10.1016/j.jmrt.2020.01.105.
[11] Sutou Y, Omori T, Kainuma R, Ono N, Ishida K. Enhancement of superelasticity in Cu-Al-Mn-Ni shape-memory alloys by texture control. Metall Mater Trans A. 2002;33(9):2817–24. doi: 10.1007/s11661-002-0267-2.
[12] Sun M, Balagurov A, Bobrikovc I, Wanga XP, Wen W, Golovinf IS, et al. High damping in Fe-Ga-La alloys: Phenomenological model for magneto-mechanical hysteresis damping and experiment. J Mater Sci Technol. 2021;72:69–80. doi: 10.1016/j.jmst.2020.07.043.
[13] Sari U, Kirindi T, Ozcan F, Dikici M. Effects of aging on the microstructure of a Cu-Al-Ni-Mn shape memory alloy. Int J Min Metall Mater. 2011;18(4):430–6. doi: 10.1007/s12613-011-0458-1.
[14] Saud SN, Bakar TA, Hamzah E, Ibrahim MK, Bahador A. Effect of quarterly element addition of cobalt on phase transformation characteristics of Cu-Al-Ni shape memory alloys. Metall Mater Trans A. 2015;46(8):3528–42. doi: 10.1007/s11661-015-2924-2.
[15] Dong QY, Shen LN, Wang MP, Jia YL, Li Z, Cao F, et al. Microstructure and properties of Cu-2.3Fe-0.03P alloy during thermomechanical treatments. Trans Nonferr Met Soc. 2015;25(5):1551–8. doi: 10.1016/S1003-6326(15)63757-8.
[16] Zhang QM, Cui B, Sun B, Zhang X, Dong ZZ, Liu QS, et al. Effect of Sm doping on the microstructure, mechanical properties and shape memory effect of Cu-13.0Al-4.0Ni alloy. Materials. 2021;14(14):4007. doi: 10.3390/ma14144007.
[17] Kalinga T, Murigendrappa SM, Kattimani S. Pseudoelastic behavior of oron-doped β_1-Type Cu-Al-Be shape memory alloys. J Mater Eng Perform. 2021;30(8):6068–78. doi: 10.1007/s11665-021-05825-x.
[18] Mallik US, Sampath V. Effect of composition and ageing on damping characteristics of Cu-Al-Mn shape memory alloys. Mater Sci Eng A. 2008;478(1–2):48–55. doi: 10.1016/j.msea.2007.05.073.
[19] Jiao Z, Wang QZ, Yin FX, Cui CX. Effect of precipitation during parent phase aging on the microstructure and properties of a refined CuAlMn shape memory alloy. Mater Sci Eng A. 2018;737:124–31. doi: 10.1016/j.msea.2018.09.037.
[20] Liu QL, Li M, Gu YZ, Wang SK, Zhang YY, Li QW, et al. Interlocked CNT networks with high damping and storage modulus. Carbon. 2015;86:46–53. doi: 10.1016/j.carbon.2015.01.014.
[21] Sutou Y, Omori T, Kainuma R, Ishida K. Ductile Cu-Al-Mn based shape memory alloys: general properties and applications. Mater Sci Tech-lond. 2008;24(8):896–901. doi: 10.1179/174328408X302567.
[22] Saud SN, Hamzah E, Abubakar T, Farahany S, Bakhsheshi-Rad HR. Effects of quenching media on phase transformation characteristics and hardness of Cu-Al-Ni-Co shape memory alloys. J Mater Eng Perform. 2015;24(4):1522–30. doi: 10.1007/s11665-015-1436-y.
[23] Pandey A, Hussain S, Nair P, Dasgupta R. Influence of niobium and silver on mechanical properties and shape memory behavior of Cu-12Al-4Mn alloys. J Alloy Compd. 2020;836:155266. doi: 10.1016/j.jallcom.2020.155266.
[24] Adorno AT, Silva RAG. Ageing behavior in the Cu-10wt%Al and Cu-10wt%Al-4wt%Ag alloys. J Alloy Compd. 2009;473(1–2):139–44. doi: 10.1016/j.jallcom.2008.05.072.
[25] Kainuma R, Takahashi S, Ishida K. Thermoelastic martensite and shape memory effect in ductile Cu-Al-Mn alloys. Metall Mater Trans A. 1996;27:2187–95. doi: 10.1007/BF02651873.
[26] Wang GQ, Liu Y, Ren GC, Zhan ZK. Analyzing as-cast age hardening of 356 cast alloy. J Mater Eng Perform. 2011;20(3):399–404. doi: 10.1007/s11665-010-9708-z.
[27] Yi DW, Xing JD, Ma SQ, Fu HG, Chen W, Li YF, et al. Three-body abrasive wear behavior of low carbon Fe-B cast alloy and its microstructures under different casting process. Tribol Lett. 2011;42(1):67–77. doi: 10.1007/s11249-011-9748-z.
[28] Bao CL, Zhang SQ, Ren YY, Zhang YW, Xie HS, Zhao J. Research progress on refractory composition and deformability of shell molds for TiAl alloy castings. China Foundry. 2018;15(1):1–10. doi: 10.1007/s41230-018-7022-9.
[29] Leu SS, Chen YC, Jean RD. Effect of rapid solidification on mechanical properties of Cu-Al-Ni shape memory alloys. J Mater Sci. 1992;27(10):2792–8. doi: 10.1007/BF00540706.
[30] Duerig TW, Albrecht J, Gessinger GH. A shape-memory alloy for high-temperature applications. JOM. 1982;34(12):14–20. doi: 10.1007/BF03338156.
[31] Agrawal A, Dube RK. Methods of fabricating Cu-Al-Ni shape memory alloys. J Alloy Compd. 2018;750:235–47. doi: 10.1016/j.jallcom.2018.03.390.
[32] Wang XJ, Zhu SM, Easton MA, Gibson MA, Savage G. Heat treatment of vacuum high pressure die cast magnesium alloy AZ91. Int J Cast Met Res. 2014;27(3):161–6. doi: 10.1179/1743133613Y.0000000091.
[33] Lee JS, Wayman CM. Grain refinement of a Cu-Al-Ni shape memory alloy by Ti and Zr additions. Trans Jpn Inst Met. 1986;27:584–91. doi: 10.2320/matertrans1960.27.584.
[34] Chen ZW, Li SS, Zhao J. Homogenization of twin-roll cast A8006 alloy. T Nonferr Met Soc. 2012;22(6):1280–5. doi: 10.1016/S1003-6326(11)61316-2.
[35] Sueyoshi H, Ishii R, Fukudome H, Mizokuchi S, Wakabayashi T, Saikusa K. Properties of soldering Cu/Fe alloy produced by powder metallurgy. J Jpn Inst Met Mater. 2009;73(6):414–20. doi: 10.2320/jinstmet.73.414.
[36] Kumara N, Bhartia A, Saxena KK. A re-investigation: effect of powder metallurgy parameters on the physical and mechanical properties of aluminium matrix composites. Mater Today Proc. 2021;44:2188–93. doi: 10.1016/j.matpr.2020.12.351.
[37] Qu ZH, Zhang PX, Liang SJ, Lai YJ, Luo C. Deformation behavior of superalloy powder compact under hot isostatic pressing. Adv Eng Mater. 2020;22:2000534. doi: 10.1002/adem.202000534.
[38] Suryanarayana C. Mechanical alloying and milling. Prog Mater Sci. 2001;46:1–184. doi: 10.1016/S0079-6425(99)00010-9.

[39] Vajpai SK, Dube RK, Sangal S. Application of rapid solidification powder metallurgy processing to prepare Cu-Al-Ni high temperature shape memory alloy strips with high strength and high ductility. Mater Sci Eng A. 2013;570:32–42. doi: 10.1016/j.msea.2013.01.063.
[40] Shafeeq M, Gupta GK, Hirshikesh, Malik MM, Modi OP. Effect of milling parameters on processing, microstructure and properties of Cu-Al-Ni-Ti shape memory alloys. Powder Metall. 2015;58(4):265–72. doi: 10.1179/1743290115Y.0000000002.
[41] Lei RS, Wang MP, Li Z, Wei HG, Yang WC, Jia YL, et al. Structure evolution and solid solubility extension of copper-niobium powders during mechanical alloying. Mater Sci Eng A. 2011;528(13–14):4475–81. doi: 10.1016/j.msea.2011.02.083.
[42] Botcharova E, Heilmaier M, Freudenberger J, Drew G, Kudashow D, Martin U, et al. Supersaturated solid solution of niobium in copper by mechanical alloying. J Alloy Compd. 2003;351(1–2):119–25. doi: 10.1016/S0925-8388(02)01025-3.
[43] Yue H, Yao L, Xin G, Zhang S, Zhang H, Guo E. Effect of ball-milling and graphene contents on the mechanical properties and fracture mechanisms of graphene nanosheets reinforced copper matrix composites. J Alloy Compd. 2017;691:755–62. doi: 10.1016/j.jallcom.2016.08.303.
[44] Shu R, Jiang XS, Shao ZY, Sun DM, Zhu DG, Luo ZP. Fabrication and mechanical properties of MWCNTs and graphene synergetically reinforced Cu-graphite matrix composites. Powder Technol. 2019;349:59–69. doi: 10.1016/j.powtec.2019.03.021.
[45] Mayahi R, Shokuhfar A, Vaezi MR. Microstructure and thermodynamic analysis of nanostructured Cu-13.2%Al-4%Ni ternary system synthesized by mechanical alloying. Metall Res Technol. 2019;116(6):628. doi: 10.1051/metal/2019056.
[46] Su Y, Li Z, Yu Y, Zhao L, Li ZL, Guo Q, et al. Composite structural modeling and tensile mechanical behavior of graphene reinforced metal matrix composites. Sci China Mater. 2018;61(1):112–24. doi: 10.1007/s40843-017-9142-2.
[47] Deng Z, Yin HQ, Zhang C, Zhang GF, Li WQ, Zhang T, et al. Microstructure and mechanical properties of Cu-12Al-xNi alloy prepared using powder metallurgy. Mater Sci Eng A. 2019;759:241–51. doi: 10.1016/j.msea.2019.05.051.
[48] Zaara K, Chemingui M, Optasanu V, Khitouni M. Solid solution evolution during mechanical alloying in Cu-Nb-Al compounds. Int J Min Met Mater. 2019;26(9):1129–39. doi: 10.1007/s12613-019-1820-y.
[49] Abedinzadeh R, Safavi SM, Karimzadeh F. A study of pressureless microwave sintering, microwave-assisted hot press sintering and conventional hot pressing on properties of aluminium/alumina nanocomposite. J Mech Sci Technol. 2016;30(5):1967–72. doi: 10.1007/s12206-016-0402-4.
[50] Wang YH, Lin JP, Yue-Hui HE, Yan L, Lin Z, Chen GL. Reaction mechanism in high Nb containing TiAl alloy by elemental powder metallurgy. T Nonferr Met Soc. 2006;16(4):853–7. doi: 10.1016/S1003-6326(06)60339-7.
[51] Xiao Z, Zhou L, Mei F, Xiong SY, Sheng XF, zhou MQ. Effect of processing of mechanical alloying and powder metallurgy on microstructure and properties of Cu-Al-Ni-Mn alloy. Mater Sci Eng A. 2008;488(1–2):266–72. doi: 10.1016/j.msea.2007.11.037.
[52] Liu JW, Li Y, Lu SQ, Wan J, Gao WL. Study on the process characteristics of vacuum hot pressing sintering of TiNiNb alloy based on “near net shape forming”. Mater Lett. 2021;294:129758. doi: 10.1016/j.matlet.2021.129758.
[53] Rodríguez PP, Ibarra A, Iza-Mendia A, Recarte V, Perez-Landazabal JI, San Juan J, et al. Influence of thermo-mechanical processing on the microstructure of Cu-based shape memory alloys produced by powder metallurgy. Mater Sci Eng A. 2004;378:263–8. doi: 10.1016/j.msea.2003.09.117.
[54] Vajpai SK, Dube RK, Sangal S. Microstructure and properties of Cu-Al-Ni shape memory alloy strips prepared via hot densification rolling of argon atomized powder preforms. Mater Sci Eng A. 2011;529:378–87. doi: 10.1016/j.msea.2011.09.046.
[55] Zhou J, Duszczyk J. Liquid phase sintering of an AA2014-based composite prepared from an elemental powder mixture. J Mater Sci. 1999;34(3):545–50. doi: 10.1023/A:1004594628862.
[56] Wakai F, Yoshida M, Shinoda Y, Akatsu T. Coarsening and grain growth in sintering of two particles of different sizes. Acta Mater. 2005;53(5):1361–71. doi: 10.1016/j.actamat.2004.11.029.
[57] Wang GF, Yang JL, Jiao XY. Microstructure and mechanical properties of Ti-22Al-25Nb alloy fabricated by elemental powder metallurgy. Mater Sci Eng A. 2016;654(27):69–76. doi: 10.1016/j.msea.2015.12.037.
[58] Ran G, Zhou J, Wang QG. The effect of hot isostatic pressing on the microstructure and tensile properties of an unmodified A356-T6 cast aluminum alloy. J Alloy Compd. 2006;421(1-2):80–6. doi: 10.1016/j.jallcom.2005.11.019.
[59] Atkinson HV, Davies S. Fundamental aspects of hot isostatic pressing: An overview. Mater Sci Eng A. 2000;31(12):2981–3000. doi: 10.1007/s11661-000-0078-2.
[60] Loh NL, Sia KY. An overview of hot isostatic pressing. J Mater Process Technol. 1992;30(1):45–65. doi: 10.1016/0924-0136(92)90038-T.
[61] Cai C, Song B, Xue P, Wei QS, Wu JM, Li W, et al. Effect of hot isostatic pressing procedure on performance of Ti6Al4V: Surface qualities, microstructure and mechanical properties. J Alloy Compd. 2016;686:55–63. doi: 10.1016/j.jallcom.2016.05.280.
[62] Ahmed M, Savvakin DG, Ivasishin OM, Pereloma EV. The effect of cooling rates on the microstructure and mechanical properties of thermo-mechanically processed Ti-Al-Mo-V-Cr-Fe alloys. Mater Sci Eng A. 2013;576:167–77. doi: 10.1016/j.msea.2013.03.083.
[63] Chang L, Sun W, Cui Y, Yang R. Influences of hot-isostatic-pressing temperature on microstructure, tensile properties and tensile fracture mode of Inconel 718 powder compact. Mater Sci Eng A. 2014;599:186–95. doi: 10.1016/j.msea.2014.01.095.
[64] Jiang XS, Liu WX, Li YJ, Shao ZY, Luo ZP, Zhu DG, et al. Microstructures and mechanical properties of Cu/Ti3SiC2/C/graphene nanocomposites prepared by vacuum hot-pressing sintering and hot isostatic pressing. Compos Part B-Eng. 2018;141:203–13. doi: 10.1016/j.compositesb.2017.12.050.
[65] Shu R, Jiang XS, Liu WX, Shao ZY, Song TF, Luo ZP. Synergetic effect of nano-carbon and HBN on microstructure and

mechanical properties of Cu/Ti3SiC2/C nanocomposites. Mater Sci Eng A. 2019;755:128–37. doi: 10.1016/j.msea.2019.04.002.
[66] Chang JC, Choi C, Kim JC, Yun YH. Development of microstructure and mechanical properties of a Ni-base single-crystal superalloy by hot-isostatic pressing. J Mater Eng Perform. 2003;12(4):420–5. doi: 10.1361/105994903770342953.
[67] Xuan W, Ren Z. Mechanism of improved intermediate temperature plasticity of nickel-base single crystal superalloy with hot isostatic pressing. J Mater Res Technol. 2021;14:673–6. doi: 10.1016/j.jmrt.2021.07.010.
[68] Durowoju MO, Sadiku ER, Diouf S, Shongwe MB, Olubambi PA. Spark plasma sintering of graphite-aluminum powder reinforced with SiC/Si particles. Powder Technol. 2015;284:504–13. doi: 10.1016/j.powtec.2015.07.027.
[69] Bustillos J, Lu XL, Nautiyal P, Zhang C, Boesl B, Agarwal A. Boron nitride nanotube-reinforced titanium composite with controlled interfacial reactions by spark plasma sintering. Adv Eng Mater. 2020;22:2000702. doi: 10.1002/adem.202000702.
[70] Kashkarov EB, Syrtanov MS, Sedanova EP, Ivashutenko AS, Lider AM, Travitzky N. Fabrication of paper-derived Ti3SiC2-based materials by spark plasma sintering. Adv Eng Mater. 2020;22:2000136. doi: 10.1002/adem.202000136.
[71] Zhang F, Reich M, Kessler O, Burkel E. The potential of rapid cooling spark plasma sintering for metallic materials. Mater Today. 2013;16(5):192–7. doi: 10.1016/j.mattod.2013.05.005.
[72] Saheb N, Iqbal Z, Khalil A, Hakeem AS, Aqeeli NA, Laoui T, et al. Spark plasma sintering of metals and metal matrix manocomposites: a review. J Nanomater. 2012;2012:983470. doi: 10.1155/2012/983470.
[73] Goupil G, Bonnefont G, Idrissi H, Daniel GY, Roué L. Consolidation of mechanically alloyed Cu-Ni-Fe material by spark plasma sintering and evaluation as inert anode for aluminum electrolysis. J Alloy Compd. 2013;580:256–61. doi: 10.1016/j.jallcom.2013.05.128.
[74] Richard A, Portier, Ochin P, Pasko A, Monastyrsky GE, Gilchuk AV, et al. Spark plasma sintering of Cu-Al-Ni shape memory alloy. J Alloy Compd. 2013;577(1):S472–7. doi: 10.1016/j.jallcom.2012.02.145.
[75] Eze AA, Jamiru T, Sadiku ER, Durowoj MO, Kupolati WK, Ibrahim ID, et al. Effect of titanium addition on the microstructure, electrical conductivity and mechanical properties of copper by using SPS for the preparation of Cu-Ti alloys. J Alloy Compd. 2018;736:163–71. doi: 10.1016/j.jallcom.2017.11.129.
[76] Qiang F, Kang ZX, Can YW, Long Y. Microstructures and mechanical properties of spark plasma sintered Cu-Cr composites prepared by mechanical milling and alloying. Mater Des. 2015;88(25):8–15. doi: 10.1016/j.matdes.2015.08.127.
[77] Tan W, Huang L, Li S, He J. Microstructure and mechanical properties of Zr-Al-Ni-Cu Metallic glassy particles reinforced 7056Al alloy matrix composites obtained by spark plasma sintering. Adv Eng Mater. 2019;21(6):1801267. doi: 10.1002/adem.201801267.
[78] Manière C, Lee G, Olevsky EA. All-materials-inclusive flash spark plasma sintering. Sci Rep. 2017;7(1):15071. doi: 10.1038/s41598-017-15365-x.
[79] Bustillos J, Zhang C, Loganathan A, Boesl B, Agarwal A. Ultralow temperature densification of a titanium alloy by spark plasma sintering. Adv Eng Mater. 2020;22:2000076. doi: 10.1002/adem.202000076.
[80] Mazzer EM, Kiminami CS, Bolfarini C, Cava RD, Botta WJ, Gargarella P, et al. Phase transformation and shape memory effect of a Cu-Al-Ni-Mn-Nb high temperature shape memory alloy. Mater Sci Eng A. 2016;663:64–8. doi: 10.1016/j.msea.2016.03.017.
[81] Saud SN, Hamzah E, Abubakar T, Bakhsheshi-Rad HR. Influence of silver nanoparticles addition on the phase transformation, mechanical properties and corrosion behaviour of Cu-Al-Ni shape memory alloys. J Alloy Compd. 2014;612:471–8. doi: 10.1016/j.jallcom.2014.05.173.
[82] Sari U. Influences of 2.5wt%Mn addition on the microstructure and mechanical properties of Cu-Al-Ni shape memory alloys. Int J Min Met Mater. 2010;17(2):192–8. doi: 10.1007/s12613-010-0212-0.
[83] Bracey CL, Ellis PR, Hutchings GJ. Application of copper-gold alloys in catalysis: current status and future perspectives. Chem Soc Rev. 2009;38(8):2231–43. doi: 10.1039/b817729p.
[84] Zuo X, Qu L, Zhao C, An B, Wang E, Niu R, et al. Nucleation and growth of γ-Fe precipitate in Cu-2%Fe alloy aged under high magnetic field. J Alloy Compd. 2016;662:355–60. doi: 10.1016/j.jallcom.2015.12.046.
[85] Dasgupta R, Jain AK, Kumar P, Hussain S, Pandey A. Role of alloying additions on the properties of Cu-Al-Mn shape memory alloys. J Alloy Compd. 2015;620:60–6. doi: 10.1016/j.jallcom.2014.09.047.
[86] Lu X, Chen F, Li W, Zheng YF. Effect of Ce addition on the microstructure and damping properties of Cu-Al-Mn shape memory alloys. J Alloy Compd. 2009;480(2):608–11. doi: 10.1016/j.jallcom.2009.01.134.
[87] Wu Q, Miao WS, Zhang YD, Gao HJ, David H. Mechanical properties of nanomaterials: a review. Nanotechnol Rev. 2020;9:259–73. doi: 10.1515/ntrev-2020-0021.
[88] Saud SN, Hamzah E, Abubakar T, Ibrahim MK, Bahador A. Effect of a fourth alloying element on the microstructure and mechanical properties of Cu-Al-Ni shape memory alloys. J Mater Res. 2015;30(14):2258–69. doi: 10.1557/jmr.2015.196.
[89] Sampath V. Studies on the effect of grain refinement and thermal processing on shape memory characteristics of Cu-Al-Ni alloys. Smart Mater Struct. 2005;14(5):S253–60. doi: 10.1088/0964-1726/14/5/013.
[90] Saud SN, Hamzah E, Abubakar T, Zamri M, Tanemura M. Influence of Ti additions on the martensitic phase transformation and mechanical properties of Cu-Al-Ni shape memory alloys. J Therm Anal Calorim. 2014;118(1):111–22. doi: 10.1007/s10973-014-3953-6.
[91] Zhang X, Cui TY, Liu QS, Dong ZZ, Chen M. Effect of Nd addition on the microstructure, mechanical properties, shape memory effect and corrosion behaviour of Cu-Al-Ni high-temperature shape memory alloys. J Alloy Compd. 2020;858:157685. doi: 10.1016/j.jallcom.2020.157685.
[92] Sugimoto K, Kamei K, Matsumoto H, Komatsu S, Akamatsu K, Sugimoto T. Grain-refinement and the related phenomena in quaternary Cu-Al-Ni-Ti shape memory alloys. J Phys. 1982;43(12):761–6. doi: 10.1051/jphyscol:19824124.
[93] Sobrero CE, Roca PL, Roatta A, Bolmaro RE, Malarria J. Shape memory properties of highly textured Cu-Al-Ni-(Ti) alloys.

Mater Sci Eng A. 2012;536:207–15. doi: 10.1016/j.msea.2011.12.104.
[94] Adachi K, Shoji K, Hamada Y. Formation of X phase and origin of grain refinement effect in Cu-Al-Ni shape memory alloys added with titanium. ISIJ Int. 1989;29(5):378–87. doi: 10.2355/isijinternational.29.378.
[95] Dalvand P, Raygan S, Lopez GA, Melendez MB, Chernenko VA. Properties of rare earth added Cu-12wt%Al-3wt%Ni-0.6wt%Ti high temperature shape memory alloy. Mater Sci Eng A. 2019;754:370–81. doi: 10.1016/j.msea.2019.03.022.
[96] Abbass MK, Adnan RSA, Alkubaisy MM. Computer approach of effect of 0.3% of Ge, Te and Ce additions on thermodynamic properties and shape memory effect of Cu-14%Al-4.5%Ni shape memory alloys. Mater Today Proc. 2018;5(9):17602–10. doi: 10.1016/j.matpr.2018.06.078.
[97] Liu AL, Gao ZY, Gao L, Cai W, Wu Y. Effect of Dy addition on the microstructure and martensitic transformation of a Ni-rich TiNi shape memory alloy. J Alloy Compd. 2007;437(1–2):339–43. doi: 10.1016/j.jallcom.2006.08.006.
[98] Zhao ZQ, Xiong W, Wu SX, Wang XL. Bending strength and fracture behavior of Ni50Mn29Ga21 alloy with terbium. J Iron Steel Res Int. 2004;11(5):55–8. doi: 10.1007/s11771-004-0070-x.
[99] Yang GS, Lee JK, Jang WY. Effect of grain refinement on phase transformation behavior and mechanical properties of Cu-based alloy. Trans Nonferr Met Soc. 2009;19(4):979–83. doi: 10.1016/S1003-6326(08)60390-8.
[100] Zhang X, Sui J, Liu Q, Cai W. Effects of Gd addition on the microstructure, mechanical properties and shape memory effect of polycrystalline Cu-Al-Ni shape memory alloy. Mater Lett. 2016;180:223–7. doi: 10.1016/j.matlet.2016.05.149.
[101] Yildiz K. Influence of Ta content on martensitic transformation and shape memory properties of Cu-Al-Ni-Mn shape memory alloy. Appl Phys A-Mater. 2020;126(4):307. doi: 10.1007/s00339-020-03475-9.
[102] Zhou L, Li S, Tang QW, Deng XC, Wei KX, Ma WH. Effects of solidification rate on the leaching behavior of metallic impurities in metallurgical grade silicon. J Alloy Compd. 2021;882:160570. doi: 10.1016/j.jallcom.2021.160570.
[103] Lin G, Pan QL, Wang WY, Liu B, Huang ZQ, Xiang SQ, et al. The role of trace Sc and Y in the corrosion resistance of cold drawn Al-0.2Ce based alloys with high electrical conductivity. J Alloy Compd. 2021;882:160708. doi: 10.1016/j.jallcom.2021.160708.
[104] Shang L, Jung IH, Yue S, Verma R, Essadiqi E. An investigation of formation of second phases in microalloyed, AZ31 Mg alloys with Ca, Sr and Ce. J Alloy Compd. 2010;492:173–83. doi: 10.1016/j.jallcom.2009.11.159.
[105] Liu K, Yu HC, Li X, Wu SJ. Study on diffusion characteristics of Al-Cu systems and mechanical properties of intermetallics. J Alloy Compd. 2021;874:159831. doi: 10.1016/j.jallcom.2021.159831.
[106] Li MH, Gao XH, Wu JJ, Wei HX, Luo HQ, Song WL. The application and comparison of EPMA WDS and EDS in material analysis. J Chin Electron Microsc Soc. 2020;39:218–23. doi: 10.3969/j.issn.1000-6281.2020.02.018.
[107] Wu YY, Li LX, Hu XJ. The analysis methods and applications of EPMA in materials. J Chin Electron Microsc Soc. 2010;29:574–7. doi: 10.3969/j.issn.1000-6281.2010.06.014.
[108] Xiao P, Gao YM, Xu FX, Yang SS, Li B, Li YF, et al. An investigation on grain refinement mechanism of TiB2 particulate reinforced AZ91composites and its effect on mechanical properties. J Alloy Compd. 2018;780:237–44. doi: 10.1016/j.jallcom.2018.11.253.
[109] Fan Z, Wang Y, Zhang Y, Qin T, Zhou XR. , Thompson GE. Grain refining mechanism in the Al/Al-Ti-B system. Acta Mater. 2015;84:292–304. doi: 10.1016/j.actamat.2014.10.055.
[110] Yang CL, Zhang B, Zhao DC, Lu HB, Zhai TG, Liu F. Microstructure and mechanical properties of AlN particles in situ reinforced Mg matrix composites. Mater Sci Eng A. 2016;674:158–63. doi: 10.1016/j.msea.2016.07.056.
[111] Ding YJ, Wang QZ, Yin FX, Cui CX, Hao GL. Effect of combined addition of Cu51Zr14 inoculant and Ti element on the microstructure and damping behavior of a Cu-Al-Ni shape memory alloy. Mater Sci Eng A. 2019;743:606–10. doi: 10.1016/j.msea.2018.11.124.
[112] Zhang X, Liu QS. Influence of Alloying Element Addition on Cu-Al-Ni high-temperature shape memory alloy without second phase formation. Acta Metall Sin. 2016;29(9):884–8. doi: 10.1007/s40195-016-0467-1.
[113] Li YY, Wang JM, Jiang CB. Study of Ni-Mn-Ga-Cu as single-phase wide-hysteresis shape memory alloys. Mater Sci Eng A. 2011;528(22–23):6907–11. doi: 10.1016/j.msea.2011.05.060.
[114] Adnan RS, Abbass MK, Alkubaisy MM. Effect of Ce addition on mechanical properties and shape memory effect of Cu-14%Al-4.5%Ni shape memory alloy. Mater Today Proc. 2019;20:45260. doi: 10.1016/j.matpr.2019.09.164.
[115] Wang LW, Xin JC, Cheng LJ, Zhao K, Sun BZ, Li JR, et al. Influence of inclusions on initiation of pitting corrosion and stress corrosion cracking of X70 steel in near-neutral pH environment. Corros Sci. 2019;147:108–27. doi: 10.1016/j.corsci.2018.11.007.
[116] Quested TE, Greer AL. The effect of the size distribution of inoculant particles on as-cast grain size in aluminium alloys. Acta Mater. 2004;52(13):3859–68. doi: 10.1016/j.actamat.2004.04.035.
[117] Chen ZN, Kang HJ, Fan GH, Li JH, Lu YP, Jie JC, et al. Grain refinement of hypoeutectic Al-Si alloys with B. Acta Mater. 2016;120:168–78. doi: 10.1016/j.actamat.2016.08.045.
[118] Wang Y, Xia M, Fan Z, Zhou X, Thompson GE. The effect of Al8Mn5 intermetallic particles on grain size of as-cast Mg-Al-Zn AZ91D alloy. Intermetallics. 2010;18(8):1683–9. doi: 10.1016/j.intermet.2010.05.004.
[119] Han YF, Dai YB, Wang J, Shu D, Sun BD. First-principles calculations on Al/AlB2 interfaces. Appl Surf Sci. 2011;257(17):7831–6. doi: 10.1016/j.apsusc.2011.04.038.
[120] Ueland SM, Schuh CA. Transition from many domain to single domain martensite morphology in small-scale shape memory alloys. Acta Mater. 2013;61(15):5618–25. doi: 10.1016/j.actamat.2013.06.003.
[121] Gong JH, Miao HZ, Zhao Z, Guan ZD. Effect of TiC particle size on the toughness characteristics of Al2O3-TiC composites. Mater Lett. 2001;49:235–8. doi: 10.1016/S0167-577X(00)00376-1.
[122] Wang CN, Lin HS, Hsueh MH, Wang YH, Vu TH, Lin TF. The sustainable improvement of manufacturing for nano-titanium. Sustainability. 2016;8(402):1–13. doi: 10.3390/su8040402.

[123] Qader IN, Kok M, Dadelen F. Effect of heat treatment on thermodynamics parameters, crystal and microstructure of (Cu-Al-Ni-Hf) shape memory alloy. Phys B. 2019;553:1–5. doi: 10.1016/j.physb.2018.10.021.
[124] Recarte V, Pérez-Sáez RB, Bocanegra EH, Nó ML, Juan JS. Dependence of the martensitic transformation characteristics on concentration in Cu-Al-Ni shape memory alloys. Mater Sci Eng A. 1999;273:380–4. doi: 10.1016/S0921-5093(99)00302-0.
[125] Kato H, Yasuda Y, Sasaki K. Thermodynamic assessment of the stabilization effect in deformed shape memory alloy martensite. Acta Mater. 2011;59(10):3955–64. doi: 10.1016/j.actamat.2011.03.021.
[126] Chang SH, Liao BS, Gholami-Kermanshahi M. Effect of Co additions on the damping properties of Cu-Al-Ni shape memory alloys. J Alloy Compd. 2020;847:156560. doi: 10.1016/j.jallcom.2020.156560.
[127] Shafeeq MM, Gupta GK, Malik MM, Sampath V, Modi OP. Influence of quenching methods on martensitic transformation and mechanical properties of P/M processed Cu-Al-Ni-Ti shape memory alloys. Powder Metall. 2016;59(4):271–80. doi: 10.1080/00325899.2016.1206261.
[128] Mallik US, Sampath V. Influence of quaternary alloying additions on transformation temperatures and shape memory properties of Cu-Al-Mn shape memory alloy. J Alloy Compd. 2009;469(1–2):156–63. doi: 10.1016/j.jallcom.2008.01.128.
[129] Waitz T, Antretter T, Fischer FD, Simha NK, Karnthaler HP. Size effects on the martensitic phase transformation of NiTi nanograins. J Mech Phys Solids. 2007;55(2):419–44. doi: 10.1016/j.jmps.2006.06.006.
[130] Wu SK, Lin HC, Chou TS. A study of electrical resistivity, internal friction and shear modulus on an aged Ti49Ni51 alloy. Acta Metall. 1990;38(1):95–102. doi: 10.1016/0956-7151(90)90137-6.
[131] Chang SH. Influence of chemical composition on the damping characteristics of Cu-Al-Ni shape memory alloys. Mater Chem Phys. 2011;125(3):358–63. doi: 10.1016/j.matchemphys.2010.09.077.
[132] Sutou Y, Omori T, Koeda N, Kainuma R, Ishida K. Effects of grain size and texture on damping properties of Cu-Al-Mn-based shape memory alloys. Mater Sci Eng A. 2006;438:743–6. doi: 10.1016/j.msea.2006.02.085.
[133] Jiao Z, Wang QZ, Yin FX, Cui CX, Zhang JJ, Yao C. Effects of Cu51Zr14 inoculant and caliber rolling on microstructures and comprehensive properties of a Cu-Al-Mn shape memory alloy. Mater Sci Eng A. 2020;772:138773. doi: 10.1016/j.msea.2019.138773.
[134] Chen MS, Wang GQ, Li HB, Lin YC, Zou ZH, Ma YY. Annealing treatment methods and mechanisms for refining mixed and coarse grains in a solution treatment nickel-based superalloy. Adv Eng Mater. 2019;21:1900558. doi: 10.1002/adem.201900558.
[135] Zhu ZY, Chen JH, Cai YF, Li JQ, Shen Y. Effect of heat treatment on the microstructure and fracture behaviors of a Ni-Cr-Fe superalloy. Adv Eng Mater. 2020;22:1901070. doi: 10.1002/adem.201901070.
[136] Li M, Liu J, Yan S, Yan W, Shi B. Effect of aging treatment on damping capacity in Cu-Al-Mn shape memory alloy. J Alloy Compd. 2019;821:153213. doi: 10.1016/j.jallcom.2019.153213.
[137] Wang QZ, Lu DM, Cui CX, Liu WJ, Xu M, Yang J. Effects of aging on the structure and damping behaviors of a novel porous CuAlMn shape memory alloy fabricated by sintering-dissolution method. Mater Sci Eng A. 2014;615:278–82. doi: 10.1016/j.msea.2014.07.080.
[138] Wang Q, Wang LW, Kang J, Wang QZ, Su R, et al. Effects of aging and thermal cycling on the microstructure and damping behaviors of a porous CuAlMn shape memory alloy. J Mater Res Technol. 2020;9(4):7020–6. doi: 10.1016/j.jmrt.2020.05.031.
[139] Krishna SC, Abhay K. Properties and strengthening mechanisms in cold-rolled and aged Cu-3Ag-0.5Zr alloy. Metallogr Microstruc. 2014;3(4):323–7. doi: 10.1007/s13632-014-0147-3.
[140] Suresh N, Ramamurty U. Aging response and its effect on the functional properties of Cu-Al-Ni shape memory alloys. J Alloy Compd. 2008;449(1–2):113–8. doi: 10.1016/j.jallcom.2006.02.094.
[141] Humbeeck JV. Damping capacity of thermoelastic martensite in shape memory alloys. J Alloy Compd. 2003;355(1–2):58–64. doi: 10.1016/S0925-8388(03)00268-8.
[142] Ren CX, Wang Q, Hou JP, Zhang ZJ, Yang HJ, Zhang ZF. Exploring the strength and ductility improvement of Cu-Al alloys. Mater Sci Eng A. 2020;786:139441. doi: 10.1016/j.msea.2020.139441.
[143] Dalvand P, Raygan S, Lopez GA, Melendez MB, Chernenko VA. Effect of aging on the structure and transformation behavior of Cu-12Al-3.5Ni-0.7Ti-0.05RE high temperature shape memory alloy. Met Mater Int. 2020;26(9):1354–65. doi: 10.1007/s12540-019-00376-2.
[144] Yildiz K. On the influence of cooling rate in heat-treated Cu-Al-Ti-Ta high-temperature shape memory alloys. Mater Sci Eng A. 2020;773:1388601–4. doi: 10.1016/j.msea.2019.138860.
[145] Wang Q, Han F, Cui C. Effect of heat treatment on the two internal friction peaks in a Cu-Al-Mn shape memory alloy. J Alloy Compd. 2010;492(1–2):286–90. doi: 10.1016/j.jallcom.2009.11.072.
[146] Saud SN, Hamzah E, Abubakar T, Bakhsheshi-Rad HR, Hosseinian R. X-phase precipitation in aging of Cu-Al-Ni-xTi shape memory alloys and its influence on phase transition behavior. J Therm Anal Calorim. 2016;123(1):377–89. doi: 10.1007/s10973-015-4894-4.
[147] Lojen G, Anzel I, Kneissl A, Krizman A, Unterweger E, Kosec B, et al. Microstructure of rapidly solidified Cu-Al-Ni shape memory alloy ribbons. J Mater Process Technol. 2005;162–163(1):220–9. doi: 10.1016/j.jmatprotec.2005.02.196.
[148] Shivaramu L, Shivasiddaramaiah AG, Mallik US, Prashantha S. Effect of ageing on damping characteristics of Cu-Al-Be-Mn quaternary shape memory alloys. Mater Today Proc. 2017;4(10):11314–7. doi: 10.1016/j.matpr.2017.09.056.
[149] Wei ZG, Yang DZ. Behaviour of quenched-in vacancies during martensite aging in CuZnAl alloys with and without Ti addition. Mater Lett. 1996;27(4-5):171–5. doi: 10.1016/0167-577X(95)00282-0.
[150] Grgurić TH, Manasijević D, Kožuh S, Ivanić I, Anžel I, Kosec B, et al. The effect of the processing parameters on the martensitic transformation of Cu-Al-Mn shape memory alloy.

J Alloy Compd. 2018;765:664–76. doi: 10.1016/j.jallcom.2018.06.250.
[151] Mielczarek A, Kopp N, Riehemann W. Ageing effects after heat treatment in Cu-Al-Mn shape memory alloys. Mater Sci Eng A. 2009;521:182–5. doi: 10.1016/j.msea.2008.10.066.
[152] Yildiz K, Kok M. Study of martensite transformation and microstructural evolution of Cu-Al-Ni-Fe shape memory alloys. J Therm Anal Calorim. 2014;115(2):1509–14. doi: 10.1007/s10973-013-3409-4.
[153] Chentouf SM, Bouabdallah M, Cheniti H, Eberhardt A, Patoor E, Sari A. Ageing study of Cu-Al-Be hypoeutectoid shape memory alloy. Mater Charact. 2010;61(11):1187–93. doi: 10.1016/j.matchar.2010.07.009.
[154] Wang QZ, Han FS, Wang JX. Effects of quenched-in vacancies on the damping behaviour of Cu-11.9Al-2.5Mn shape memory alloy. Phys Status Solidi. 2010;202(1):72–8. doi: 10.1002/pssa.200406908.
[155] Saud SN, Hamzah E, Bakhsheshi-Rad HR, Abubakar T. Effect of Ta additions on the microstructure, damping, and shape memory behaviour of prealloyed Cu-Al-Ni shape memory alloys. Scanning. 2017;2017:1–13. doi: 10.1155/2017/1789454.
[156] Milhorato FR, Mazzer EM. Effects of aging on a spray-formed Cu-Al-Ni-Mn-Nb high temperature shape memory alloy. Mater Sci Eng A. 2019;753:232–7. doi: 10.1016/j.msea.2019.03.024.
[157] Li HZ, Wang QZ, Yin FX, Cui CX, Hao GL, Jiao ZX, et al. Effects of parent phase aging and Nb element on the microstructure, martensitic transformation, and damping behaviors of a Cu-Al-Mn shape memory alloy. Phys Status Solidi A. 2020;217(6):1900923. doi: 10.1002/pssa.201900923.
[158] Srikanth N, Thein MA, Gupta M. Effect of milling on the damping behavior of nano-structured copper. Mater Sci Eng A. 2004;366(1):38–44. doi: 10.1016/j.msea.2003.08.064.
[159] Kumar A, Tun KS, Kohadkar AD, Gupta M. Improved compressive, damping and coefficient of thermal expansion response of Mg-3Al-2.5La alloy using Y_2O_3 nano reinforcement. Metals. 2017;7(3):104. doi: 10.3390/met7030104.
[160] Hassan SF, Gupta M. Development of high performance magnesium nanocomposites using solidification processing route. Mater Sci Technol. 2004;20(11):1383–8. doi: 10.1179/026708304X3980.
[161] Ahamed H, Senthilkumar V. Role of nano-size reinforcement and milling on the synthesis of nano-crystalline aluminium alloy composites by mechanical alloying. J Alloy Compd. 2010;505(2):772–82. doi: 10.1016/j.jallcom.2010.06.139.
[162] Hassan SF, Gupta M. Effect of different types of nano-size oxide particulates on microstructural and mechanical properties of elemental Mg. J Mater Sci. 2006;41(8):2229–36. doi: 10.1007/s10853-006-7178-3.
[163] Abbass MK, Sultan BF. Influence of Al_2O_3 and SiO_2 nanoparticles on hardness and corrosion resistance of aluminum alloy(Al-4.5%Cu-1.5%Mg). Mater Res Express. 2019;6(10):1050a8. doi: 10.1088/2053-1591/ab4066.
[164] Lee J, Kim YC, Lee S, Ahn S, Kim NJ. Correlation of the microstructure and mechanical properties of oxide-dispersion-strengthened coppers fabricated by internal oxidation. Metall Mater Trans A. 2004;35A(2):493–502. doi: 10.1007/s11661-004-0360-9.
[165] Yang JH, Xiao SL, Chen YY, Xu LJ, Wang XP, Zhang DD, et al. Effects of nano-Y2O3 addition on the microstructure evolution and tensile properties of a near-alpha titanium alloy. Mater Sci Eng A. 2019;761:137977. doi: 10.1016/j.msea.2019.05.107.
[166] Ebrahimi M, Zhang L, Wang QD, Zhou H, Li WZ. Damping characterization and its underlying mechanisms in CNTs/AZ91D composite processed by cyclic extrusion and compression. Mater Sci Eng A. 2021;821:141605. doi: 10.1016/j.msea.2021.141605.
[167] Bakshi SR, Lahiri D, Agarwal A. Carbon nanotube reinforced metal matrix composites-a review. Int Mater Rev. 2010;55(1):41–64. doi: 10.1179/095066009X12572530170543.
[168] Chen FY, Ying JM, Wang YF, Du SY, Liu ZP, Huang Q. Effects of graphene content on the microstructure and properties of copper matrix composites. Carbon. 2016;96:836–42. doi: 10.1016/j.carbon.2015.10.023.
[169] Khan SU, Li CY, Siddiqui NA, Kim JK. Vibration damping characteristics of carbon fiber-reinforced composites containing multi-walled carbon nanotubes. Compos Sci Technol. 2011;71(12):1486–94. doi: 10.1016/j.compscitech.2011.03.022.
[170] Carvalho O, Miranda G, Buciumeanu M, Gasik M, Silva FS, Madeira S. High temperature damping behavior and dynamic Young's modulus of AlSi-CNT-SiCp hybrid composite. Compos Struct. 2016;141:155–62. doi: 10.1016/j.compstruct.2016.01.046.
[171] Srikanth N, Zhong XL, Gupta M. Enhancing damping of pure magnesium using nano-size alumina particulates. Mater Lett. 2005;59(29–30):3851–5. doi: 10.1016/j.matlet.2005.07.029.
[172] Severson BL, Keer LM, Ottino JM, Snurr RQ. Mechanical damping using adhesive micro or nano powders. Powder Technol. 2009;191(1–2):143–8. doi: 10.1016/j.powtec.2008.09.019.
[173] Liew KM, Kai MF, Zhang LW. Mechanical and damping properties of CNT-reinforced cementitious composites. Compos Struct. 2017;160:81–8. doi: 10.1016/j.compstruct.2016.10.043.
[174] Yu MF, Lourie O, Dyer MJ, Moloni K, Kelly TF, Ruoff RS. Strength and breaking mechanism of multiwalled carbon nanotubes under tensile load. Science. 2000;287(5453):637–40. doi: 10.1126/science.287.5453.637.
[175] Luo JL, Duan ZD, Xian GJ, Li QY, Zhao TJ. Damping performances of carbon nanotube reinforced cement composite. Mech Adv Mater Struct. 2015;22(3):224–32. doi: 10.1080/15376494.2012.736052.
[176] Chandra R, Singh S, Gupta K. Damping studies in fiber-reinforced composites-a review. Compos Struct. 1999;46(1):41–51. doi: 10.1016/S0263-8223(99)00041-0.
[177] Luo T, Zhang HL, Liu RR, Du PN, Huang ZH, Pan QF, et al. Mechanical and damping properties of the multi-layer graphenes enhanced CrMnFeCoNi high-entropy alloy composites produced by powder metallurgy. Mater Lett. 2021;293:129682. doi: 10.1016/j.matlet.2021.129682.
[178] Li JY, Chen CJ, Liao JK, Liu L, Ye XH, Lin SY, et al. Bond strengths of porcelain to cobalt-chromium alloys made by casting, milling, and selective laser melting. J Prosthet Dent. 2017;118(1):69–75. doi: 10.1016/j.prosdent.2016.11.001.

[179] Presotto AGC, Bhering CLB, Mesquita MF, Barão VAR. Marginal fit and photoelastic stress analysis of CAD-CAM and overcast 3-unit implant-supported frameworks. J Prosthet Dent. 2017;117(3):373–9. doi: 10.1016/j.prosdent.2016.06.011.

[180] Tsai DC, Hwang WS. Numerical simulation of solidification morphologies of Cu-0.6Cr casting alloy using modified cellular automaton model. T Nonferr Met Soc. 2010;20(6):1072–7. doi: 10.1016/S1003-6326(09)60260-0.

[181] Ye WL, Zhang SS, Mendez LL, Farias M, Li JZ, Xu B, et al. Numerical simulation of the melting and alloying processes of elemental titanium and boron powders using selective laser alloying. J Manuf Process. 2021;64:1235–47. doi: 10.1016/j.jmapro.2021.02.044.

[182] Wu G, Wang X, Ji C, Gao ZR, Jiang T, Zhao CX. Anti-blast properties of 6063-T5 aluminum alloy circular tubes coated with polyurea elastomer: experiments and numerical simulations. Thin-Walled Struct. 2021;164:107842. doi: 10.1016/j.tws.2021.107842.

[183] Zhou ZM, Xiao ZP, Wei BW, Hu Y, Tang LW, Liu C. The numerical simulation of rapidly solidified Cu-Cr alloys. Procedia Eng. 2012;29:3944–8. doi: 10.1016/j.proeng.2012.01.599.

[184] Akcin ET, Guncu MB, Aktas G, Aslan Y. Effect of manufacturing techniques on the marginal and internal fit of cobalt-chromium implant-supported multiunit frameworks. J Prosthet Dent. 2018;120(5):715–20. doi: 10.1016/j.prosdent.2018.02.012.

[185] Han CJ, Fang QH, Shi YS, Tor SB, Chua CK, Zhou K. Recent advances on high-entropy alloys for 3D printing. Adv Mater. 2020;32(26):1902855. doi: 10.1002/adma.201903855.

[186] Alharbi N, Wismeijer D, Osman R. Additive manufacturing techniques in prosthodontics: where do we currently stand a critical review. Int J Prosthodont. 2017;30(5):474–84. doi: 10.11607/ijp.5079.

[187] Presottoa AGC, Cordeiroa JM, Presottob JGC, Rangelc EC, Cruzc NC, Landersd R, et al. Feasibility of 3D printed Co-Cr alloy for dental prostheses applications. J Alloy Compd. 2021;865:158171. doi: 10.1016/j.jallcom.2020.158171.

[188] Zhou YN, Li N, Yan JZ, Zeng Q. Comparative analysis of the microstructures and mechanical properties of Co-Cr dental alloys fabricated by different methods. J Prosthet Dent. 2018;120(4):617–23. doi: 10.1016/j.prosdent.2017.11.015.

[189] Lawaf S, Nasermostofi S, Afradeh M, Azizi A. Comparison of the bond strength of ceramics to Co-Cr alloys made by casting and selective laser melting. J Adv Prosthodont. 2017;9(1):52–6. doi: 10.4047/jap.2017.9.1.52.

[190] Kacenkaa Z, Roudnicka M, Ekrtb O, Vojtech D. High susceptibility of 3D-printed Ti-6Al-4V alloy to hydrogen trapping and embrittlement. Mater Lett. 2021;301:130334. doi: 10.1016/j.matlet.2021.130334.